

# Simulation of Dynamic Interactions of the Earth-Air Heat Exchanger with Soil and Atmosphere for Preheating of Ventilation Air

Guohui Gan

Department of Architecture and Built Environment, University of Nottingham, University Park, Nottingham NG7 2RD, UK

Tel: +44 (0)115 9514876

guohui.gan@nottingham.ac.uk

## ABSTRACT

Earth-air tunnel ventilation is an energy efficient means of preheating and cooling of supply air to a building. Due to changing soil and atmospheric conditions and the consequent changes in heating and cooling loads of a building during operation, an earth-air heat exchanger interacts with the environments and the performance varies with the conditions. A computer program has been developed for modelling of coupled heat and moisture transfer in soil and for simulation of the thermal performance of an earth-air heat exchanger for building ventilation, taking account of dynamic variations of climatic, load and soil conditions. The importance of dynamic interactions between the three media - heat exchanger, soil and atmosphere - is illustrated from the comparison of the heat transfer rates and supply air temperature through the heat exchanger under continuous and intermittent operation in heating seasons. It is shown that neglecting the interactions between any two or all three media would significantly over or under predict the heat transfer rate and air temperature. Neglecting the interactions between the heat exchanger, soil and ventilating air would over predict the thermal performance of an earth-air heat exchanger whereas neglecting the interactions between the soil surface and atmosphere would fail to produce reliable data for long term operational performance of the earth-air heat exchanger installed in shallow ground. The level of over-prediction could be larger for intermittent operation than for continuous operation.

**KEYWORDS:** Earth-air heat exchanger, building ventilation, energy efficient heating, heat and moisture transfer, soil property, thermal interaction.

## NOMENCLATURE

b	constant dependent on the type of soil
C	specific heat of soil (J/kgK)
D	damping depth of annual temperature fluctuation (m)
$D_{T,l}$	thermal liquid diffusivities ( $m^2/sK$ )
$D_{T,v}$	vapour moisture diffusivities ( $m^2/sK$ )
$D_v$	diffusion coefficient of water vapour in air ( $m^2/s$ )
$D_{\Theta,l}$	isothermal liquid diffusivities ( $m^2/s$ )
$D_{\Theta,v}$	isothermal vapour moisture diffusivities ( $m^2/s$ )
f	ratio of the average temperature gradient of the soil constituent to that of water
$f(\Theta)$	fractional volume of gas-filled pores ( $f(\Theta) = \Theta_s - \Theta$ )
g	gravitational acceleration ( $m/s^2$ )
K	hydraulic conductivity of soil (m/s)
$K_s$	saturated hydraulic conductivity (m/s)
k	thermal conductivity of soil (W/mK)
$k_a$	thermal conductivity of dry air (W/mK)
L	latent heat of vaporisation or fusion of water (J/kg)
$p_{atm}$	atmospheric pressure (Pa)

51	$p_v$	partial pressure of water vapour (Pa)
52	$q$	specific heat extraction (W/m)
53	$q_f$	source or sink of heat at a boundary (W/m <sup>2</sup> )
54	$q_v$	volumetric heat production/dissipation rate in soil (W/m <sup>3</sup> )
55	$T$	temperature of a medium (soil) (°C)
56	$T_a$	air temperature in the heat exchanger (°C)
57	$T_{amp}$	annual amplitude of surface temperature (°C)
58	$T_m$	annual mean temperature of deep soil (°C)
59	$T_s$	temperature of the inner surface of the pipe (°C)
60	$T_v$	temperature of water vapour (°C)
61	$t$	time (s)
62	$t_o$	time lag from a starting date to the occurrence of the minimum temperature in a year
63		(day)
64	$x$	horizontal distance from pipe inlet (m)
65	$z$	vertical coordinate (m)
66	$Z$	depth from soil surface (m)
67		
68	$\alpha$	tortuosity factor for diffusion of gases in soil
69	$\Theta$	volumetric moisture content (m <sup>3</sup> /m <sup>3</sup> )
70	$\Theta_f$	source or sink of moisture at a boundary (m <sup>3</sup> /m <sup>2</sup> s)
71	$\Theta_s$	saturated volumetric moisture content (m <sup>3</sup> /m <sup>3</sup> )
72	$\Theta_v$	source or sink of moisture in soil (m <sup>3</sup> /m <sup>3</sup> s)
73	$\theta$	volumetric fraction of a constituent in soil
74	$\xi$	direction normal to a boundary
75	$\rho$	density of soil (kg/m <sup>3</sup> )
76	$\rho_l$	density of liquid (kg/m <sup>3</sup> )
77	$\rho_v$	density of water vapour (kg/m <sup>3</sup> )
78	$\rho_{vs}$	density of saturated water vapour (kg/m <sup>3</sup> )
79	$\phi$	relative humidity of soil air (fraction)
80	$\Psi$	matric potential (m)
81	$\Psi_s$	saturated matric potential (m)

82

## 83 1 INTRODUCTION

84 Earth-air tunnel ventilation has been studied and applied to buildings for decades. Properly  
85 designed and operated, the system is able to reduce the energy use for heating or cooling of a  
86 building through a ground or earth-air heat exchanger. The heat exchanger consists of a series  
87 of pipe or duct buried in the shallow ground for transferring heat between the supply air in the  
88 pipe and the surrounding soil with a relatively stable temperature. The most commonly used  
89 pipe material for a heat exchanger is plastic such as high density polyethylene.

90

91 The performance of earth-air heat exchangers can be assessed using analytical or numerical  
92 techniques or experimental measurements. Bisoniya, et al. [1] have recently reviewed  
93 experimental and analytical studies of earth-air heat exchangers worldwide but mainly in India  
94 where there has been a lot of research in this area. Analytical techniques are generally based  
95 on the simplified solution of one dimensional (axi-symmetric) heat transfer in a circular pipe  
96 or the surrounding soil of homogeneous properties. Such models range from a simple thermo-  
97 hydraulic equation for constant soil and air properties [2] to a set of analytical equations for  
98 daily and seasonally varying soil and air temperatures [3-5]. However, in earth-air tunnel  
99 ventilation, heat and moisture transfer occurs simultaneously and these transport phenomena

100 are neither axi-symmetric normal to the pipe nor varying uniformly along the pipe for long  
101 term operation due to the influence of daily and seasonal climatic variations and interactions  
102 between soil and the heat exchanger. To account for the non-uniform variations requires  
103 numerical solution of three-dimensional model equations. The numerical methods can again  
104 vary from models for heat transfer only [6-11] to those for simultaneous heat and moisture  
105 transfer [12-15] in soil. However, all these investigations have made use of some form of  
106 simplifications. For example, in the models for simultaneous heat and moisture transfer, a  
107 cylindrical coordinate system, i.e, an axi-symmetric model in horizontal direction, was used  
108 for numerical solution of the equations. Such a model would in theory not be able to  
109 differentiate boundary conditions at different positions from atmosphere to deep soil and as  
110 such the model was often applied only to part of soil surrounding the heat exchanger rather  
111 than the whole area within its influence. Besides, the heat and moisture transfer in reality is  
112 not symmetrical as will be shown from the results presented in this article. The main  
113 difference between this type of axi-symmetrical model and another even more simplistic axi-  
114 symmetric model [16] is that the former could involve the top soil boundary that links with  
115 atmospheric conditions through approximations whereas the latter was based on pure axi-  
116 symmetrical heat transfer and thus the influence of atmosphere was completely ignored. Three  
117 dimensional models had of course been developed previously, e.g. by Gauthier, et al. [11], but  
118 when used for simulation of earth-air heat exchangers, the main consideration was given to  
119 heat transfer in soil while the direct influence of moisture variation on heat transfer was  
120 neglected. This may be acceptable under the assumption of constant soil properties. However,  
121 the thermophysical properties of real soil are highly dependent on the moisture content and  
122 soil moisture could vary considerably in shallow ground. Despite its obvious shortcomings,  
123 this approach has been pursued by a number of researchers in recent years for analysis of  
124 earth-air heat exchangers using commercial software that is basically designed for modelling  
125 of general fluid flow and heat transfer rather than coupled heat and mass transfer in soil [16-  
126 20].

127

128 Three-dimensional numerical models for coupled heat and moisture transfer have nevertheless  
129 been developed for a wide range of applications from prediction of the development of caking  
130 in granular materials [21], analysis of heat, moisture, air flow and deformation in unsaturated  
131 soil [22], prediction of the moisture evolution in porous building materials [23] to assessment  
132 of the indoor thermal environment [24]. These models are generic in their own areas but  
133 modelling of an earth-air heat exchanger requires unique considerations such as interactions  
134 between the heat exchanger, soil and atmosphere which this has not been thoroughly  
135 investigated. Therefore, there is a need for a three-dimensional model that takes account of not  
136 only the coupled heat and moisture transfer in soil but also interactions between soil and  
137 atmosphere and between the heat exchanger and ventilating air in order to predict more  
138 accurately the thermal performance of an earth-air tunnel ventilation system.

139

140 The author has recently developed a more general three-dimensional numerical model for the  
141 simulation of transient heat and moisture transfer in soil with a horizontally coupled earth-air  
142 heat exchanger for preheating and cooling of buildings [25]. The mathematical model is based  
143 on the general conservation equations for heat and moisture transfer in soil. The soil is  
144 subjected to extraction/injection of heat and moisture at two types of interface. One is the  
145 ground surface where heat transfer takes place by convection, short and long wave radiation  
146 and those associated with moisture transfer due to condensation/evaporation, possible  
147 freezing/thawing and precipitation. Another is the heat exchanger buried below the ground  
148 where convection heat transfer between the inner surface and ventilating air dominates but  
149 condensation/evaporation could also occur on both the inner and outer surfaces. The model

150 thus takes account of interactions of heat and moisture transfer in soil and between the  
 151 atmosphere, soil, heat exchanger and supply air passing through the heat exchanger. It  
 152 incorporates key components for earth-air heat exchange modelling from model equations and  
 153 boundary conditions to spatial and temporal variations in soil properties and transport  
 154 processes. The model equations are solved using the control volume method and a computer  
 155 program has been developed using FORTRAN for the solution. In this article the numerical  
 156 model is outlined for simulation and then the simulated performance of an earth-air heat  
 157 exchanger is discussed for preheating of supply air in building ventilation. The consequences  
 158 of simplifying simulation or using inadequate methods for simulation on the predicted  
 159 performance are also examined and the importance of taking full account of the interactions is  
 160 demonstrated.

161

## 162 2 METHOD

163 To simulate transient heat and moisture transfer simultaneously through an earth-air heat  
 164 exchanger, a numerical method is used to solve three-dimensional energy and mass  
 165 conservation equations for soil coupled with the heat and mass balances at the two interfaces:  
 166 a) between earth and atmosphere and b) between the heat exchanger and supply air.

167

### 168 2.1 Model Equations

169 The following coupled energy and mass conservation equations describe the transient heat and  
 170 moisture transfer in soil with phase change:

$$171 \frac{\partial(\rho CT)}{\partial t} = \nabla((k + L\rho_l D_{T,v})\nabla T) + \nabla(L\rho_l D_{\Theta,v}\nabla\Theta) + q_v \quad (1)$$

$$172 \frac{\partial\Theta}{\partial t} = \nabla((D_{T,l} + D_{T,v})\nabla T) + \nabla((D_{\Theta,l} + D_{\Theta,v})\nabla\Theta) + \frac{\partial K}{\partial z} + \Theta_v \quad (2)$$

173

174 The four moisture diffusivities in the above equations are defined as follows:

$$175 D_{T,l} = K \frac{\partial\Psi}{\partial T} \quad (3)$$

$$176 D_{T,v} = D_v \alpha f(\Theta) \frac{1}{\rho_l} \frac{\partial\rho_v}{\partial T} \quad (4)$$

$$177 D_{\Theta,l} = K \frac{\partial\Psi}{\partial\Theta} \quad (5)$$

$$178 D_{\Theta,v} = D_v \alpha f(\Theta) \frac{1}{\rho_l} \frac{\partial\rho_v}{\partial\Theta} \quad (6)$$

179

180 The matric potential and hydraulic conductivity of soil are given by the following pedo-  
 181 transfer functions of moisture content [26]

$$182 \Psi = \Psi_s \left( \frac{\Theta}{\Theta_s} \right)^b \quad (7)$$

$$183 K = K_s \left( \frac{\Theta}{\Theta_s} \right)^{2b+3} \quad (8)$$

184

185 Soil is a mixture of solid matter, gases and liquids as well as living organisms. The thermal  
 186 properties of a soil mixture including the density, specific heat and thermal conductivity vary  
 187 with the composition of its constituents. They are represented by the following functions of the



188 volumetric composition of dry solid matter, gases and three phases of moisture – liquid water,  
 189 water vapour and solid ice:

$$190 \quad \rho = \rho_d \theta_d + \rho_l \theta_l + \rho_i \theta_i + \rho_p \theta_p \quad (9)$$

$$191 \quad \rho C = \rho_d C_d \theta_d + \rho_l C_l \theta_l + \rho_i C_i \theta_i + \rho_p C_p \theta_p \quad (10)$$

$$192 \quad k = \frac{k_l \theta_l + f_i k_i \theta_i + f_p k_p \theta_p + \sum_{m=1}^n f_m k_m \theta_m}{\theta_l + f_i \theta_i + k_p \theta_p + \sum_{m=1}^n f_m \theta_m} \quad (11)$$

193  
 194 In the above equations, subscripts d, l, i and p represent dry soil, liquid moisture, ice and gas-  
 195 filled pores, respectively, and m is the m<sup>th</sup> component of n types of dry soil grains.

196  
 197 The thermal conductivity of pores is influenced by dry air and the phase change of moisture:

$$198 \quad k_p = k_a + LD_v \phi \frac{P_{am}}{P_{am} - p_v} \frac{d\rho_{vs}}{dT_v} \quad (12)$$

199  
 200 The moisture in soil varies in space and time as described with Equation (2). The most  
 201 obvious change in the moisture content is often observed near the soil surface. It increases  
 202 with precipitation and condensation and decreases due to evaporation. There are however  
 203 limits for soil to hold moisture. The upper limit of moisture in soil is defined as the saturation  
 204 moisture content and the lower limit is the residual moisture content. In simulation, the  
 205 moisture content in soil at any time is set within these lower and upper limits.

206  
 207 The partial differential equations (1) and (2) are solved for a three-dimensional model using  
 208 the control volume method with the initial and boundary conditions described below. A heat  
 209 exchanger is represented by a series of parallel pipes inside a computational domain. In  
 210 practical installation, parallel pipes are connected to the external air intake and supply air  
 211 outlet through two headers of larger pipe. The size and configuration of the headers and  
 212 associated piping to the above-ground environments depend on the design of both a building  
 213 and the ventilation system including the ground heat exchanger and thus vary from one design  
 214 to another. Therefore, these components are not modelled in this work. Fig. 1 shows a  
 215 schematic diagram of the heat exchanger and the boundary conditions for simulation.

216

## 217 **2.2 Initial Conditions**

218 Empirical expressions are available that represent the annual variation of the soil temperature.  
 219 The following expression is used to set the initial soil temperature and the far-field  
 220 temperature at any time t (day) and depth,

$$221 \quad T = T_m - T_{amp} e^{-Z/D} \sin\left((t - t_o) \frac{2\pi}{365} - \frac{Z}{D} - \frac{\pi}{2}\right) \quad (13)$$

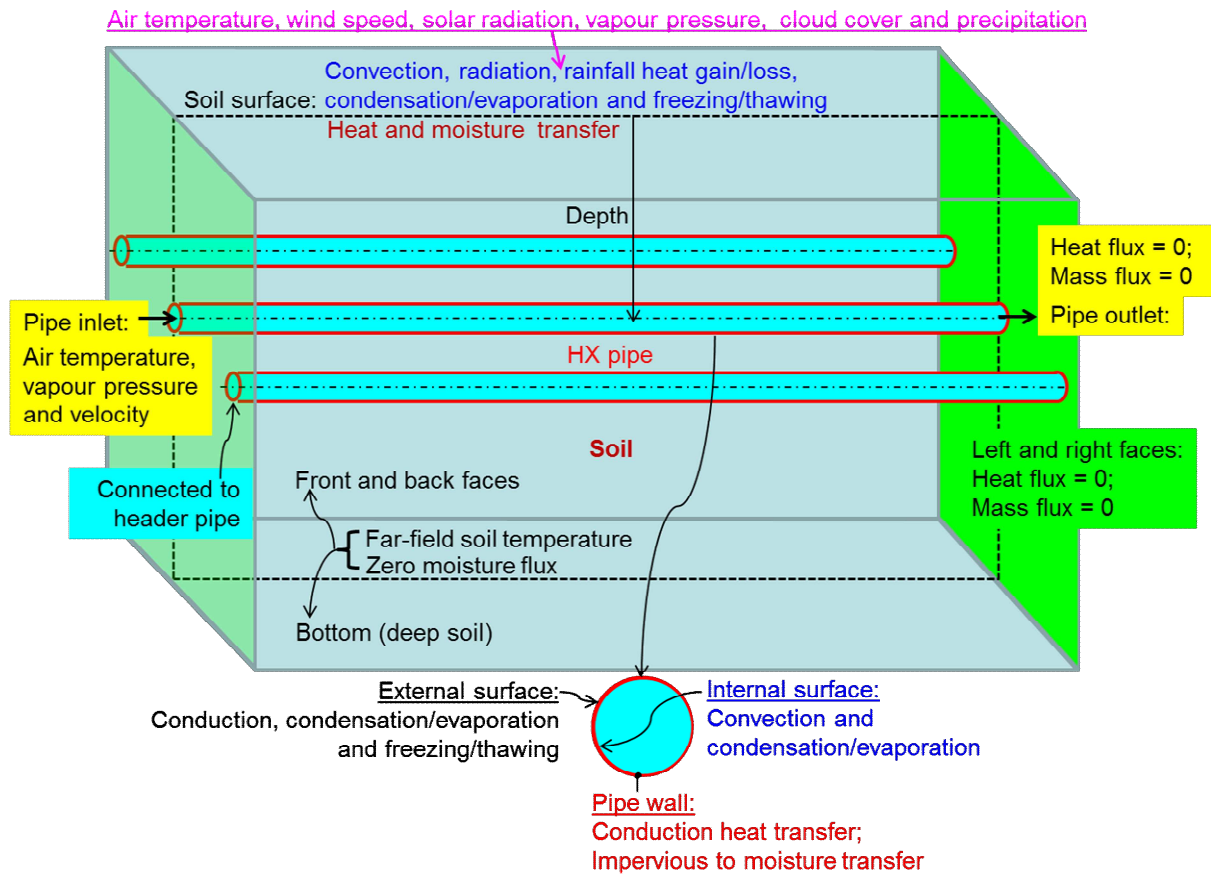
222

223 Such an expression is however not available for moisture variation in soil. It is assumed  
 224 therefore that at the beginning of simulation the soil moisture content is uniform.

225

## 226 **2.3 Boundary Conditions**

227 Boundary conditions for the solution of the three-dimensional heat and moisture transfer  
 228 equations include heat and moisture transfer for the ground or top soil surface, the bottom  
 229 face, four vertical faces, the inlet and outlet openings, and the interior and exterior surfaces of  
 230 the heat exchanger pipe.



232

233 Fig. 1 Boundary conditions for simulation of heat and moisture transfer through an earth-air  
 234 heat exchanger

235

236 For areas where soil is directly exposed to the environment or in direct contact with other  
 237 types of material/medium, i.e., the top soil surface or outer surface of the heat exchanger pipe,  
 238 the boundary conditions are given by the heat and mass balances for a control volume with a  
 239 thickness of  $\delta\xi$

240 
$$(k + L\rho_l D_{T,v}) \frac{\partial T}{\partial \xi} + L\rho_l D_{\Theta,v} \frac{\partial \Theta}{\partial \xi} = q_f \quad (14)$$

241 
$$(D_{T,l} + D_{T,v}) \frac{\partial T}{\partial \xi} + (D_{\Theta,l} + D_{\Theta,v}) \frac{\partial \Theta}{\partial \xi} = \Theta_f \quad (15)$$

242

243 The term on the right hand side represents the net heat (mass) flow into the control volume  
 244 resulting from the sources given in Table 1.

245

246 Table 1 Sources of heat and moisture flow at the soil surface and outer pipe surface

Type of boundary	Heat flow ( $q_f$ )	Moisture flow ( $\Theta_f$ )
Top soil surface	<ul style="list-style-type: none"> <li>• Short and long wave radiation</li> <li>• Wind and buoyancy induced convection</li> <li>• Moisture evaporation or condensation</li> <li>• Sensible heat from precipitation</li> </ul>	<ul style="list-style-type: none"> <li>• Evaporation or condensation</li> <li>• Precipitation</li> </ul>
Outer pipe surface	Zero	Zero

247  
248  
249  
250  
251  
252  
253  
254  
255  
256

For other surfaces, the boundary conditions are summarized in Table 2. A complete description of the boundary conditions is given in references [25 and 27].

At times when incoming air temperature is higher than the pipe temperature such that preheating of supply air is not possible or during the times when the system is switched off for intermittent operation, the inlet opening is prescribed with zero heat and mass flux for continuous simulation of heat and moisture transfer in soil.

Table 2 Boundary conditions for heat and moisture transfer

Type of boundary	Heat transfer	Moisture transfer
Far-field – vertical faces and bottom face	Equation (13)	Zero mass flux
Pipe inlet	Ambient air temperature and Ventilation rate (or velocity)	Vapour pressure (or relative humidity)
Pipe outlet	Zero heat flux	Zero mass flux
Inner pipe surface – ventilating air	Advective and conductive heat transfer → Convection + Condensation (evaporation)	Convective and diffusive moisture transfer → Condensation (evaporation)

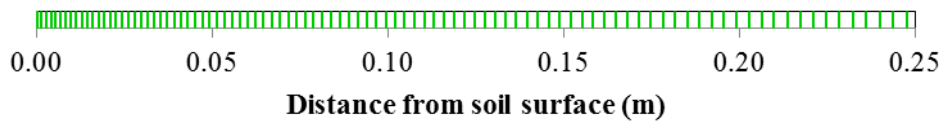
257  
258  
259  
260  
261  
262  
263  
264  
265  
266  
267  
268  
269  
270  
271  
272  
273  
274  
275  
276  
277  
278  
279  
280  
281  
282  
283  
284  
285  
286

## 2.4 Solution method

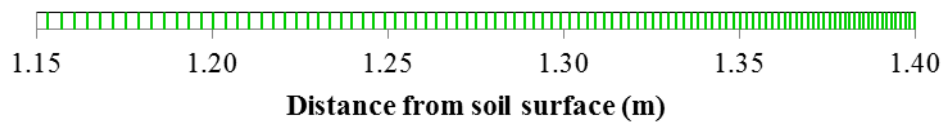
The partial differential equations for the coupled heat and moisture transfer are solved using the control volume method. This involves firstly decomposing a three-dimensional computational domain into numerous hexahedral control volumes or cells. Each partial differential equation is then integrated over each of the control volumes to obtain an integral equation. Next, the integral equation is discretised into an algebraic equation, one equation for one control volume, and the total number of algebraic equations is equal to the product of the number of variables (soil temperature and moisture) and the number of control volumes. Finally, all the algebraic equations are solved iteratively for given initial and boundary conditions some of which, e.g., Equations (14) and (15), are dependent on the outcomes of the iteration. The solution is considered to have converged when the sum of the normalised residual for each variable for the whole domain is less than  $10^{-3}$  and more importantly changes in both the residual and variables between iterations become negligible. Because the equations are highly non-linear, under relaxation is used to achieve a converged solution; the required under-relaxation factors could be as small as 0.1 at the beginning, whenever the system is switched on or off for intermittent operation, or when the heat transfer rate through the heat exchanger is high.

The size of the computational domain is such that at the end of the operating period under simulation the influence of the variations of the key variables would not reach the far-field, i.e., bottom, front and back faces denoted in Fig. 1. For simulation of one month's operation, a distance of 5 m from the heat exchanger would be sufficient. A larger domain is however used in this work to ensure that the above requirement is met, e.g., a total depth of 10 m in the vertical direction. A non-uniform mesh is used for such a large computational domain. Previous work by the author has shown the importance of using fine meshes and time steps for accurate simulation of heat and moisture transfer particularly with varying environmental conditions [25, 27 and 28]. The edge size is about 1 mm for cells close to the heat exchanger and the soil surface where potential variations in the heat and/or moisture transfer are large and the size increases gradually away from these areas to avoid the need for an excessive

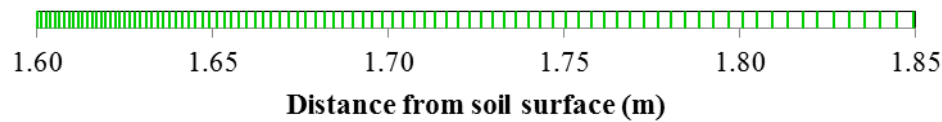
287 number of cells. Fig. 2 shows the distribution of cells in the depth direction through the  
 288 centreline of the heat exchanger for three small sections – a) starting from the soil surface  
 289 downwards, b) from the crown of the pipe upwards and c) from the bottom of the pipe  
 290 downwards – and for the whole depth where only one in 14 cells are included.  
 291



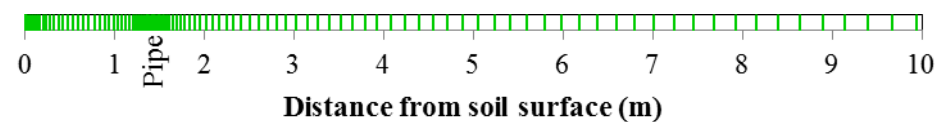
292 a) Near the soil surface  
 293  
 294



295 b) Near the crown of the pipe  
 296  
 297



298 c) Near the bottom of the pipe  
 299  
 300



301 (d) For the full depth of the domain with one in 14 cells shown  
 302  
 303

304 Fig. 2 Cell distribution in vertical direction  
 305

306 The model has been validated for simulation of transient heat transfer for preheating of supply  
 307 air through a straight pipe of 200 mm external diameter buried 1.5 m below the ground for an  
 308 ambient air temperature of 5°C and an initial deep soil temperature of 10°C [25] and for  
 309 refrigerant flow in a 40 mm diameter slinky heat exchanger [29].  
 310

311 In order to confirm the accuracy of the in-house program, further validation has been carried  
 312 out through comparison of predicted heat transfer with that using commercial software  
 313 FLUENT [30] which had been validated with experimental measurements [29]. The  
 314 conditions for validation presented here are the same as for the previous work [25] except that  
 315 the ambient air temperature is reduced from 5°C to 1°C for winter application. Detailed  
 316 conditions are as follows:

- 317 • Heat exchanger pipe = 200 mm external diameter; depth of installation = 1.5 m.
- 318 • Soil density = 1588 kg/m<sup>3</sup>; specific heat = 1465 J/kgK; thermal conductivity = 1.24  
 319 W/mK, all based on measurements [29].
- 320 • Deep soil temperature = 10°C.
- 321 • Ambient air temperature = 1°C; wind speed = 4 m/s; mean air velocity in the pipe = 2  
 322 m/s.

323 The predicted heat transfer rate per unit length of the heat exchanger is compared in Fig. 3.  
 324 Good agreement between the two sets of results can be observed with a maximum difference  
 325 of about 0.8% and average difference of less than 0.2% during a period of 30 days.  
 326

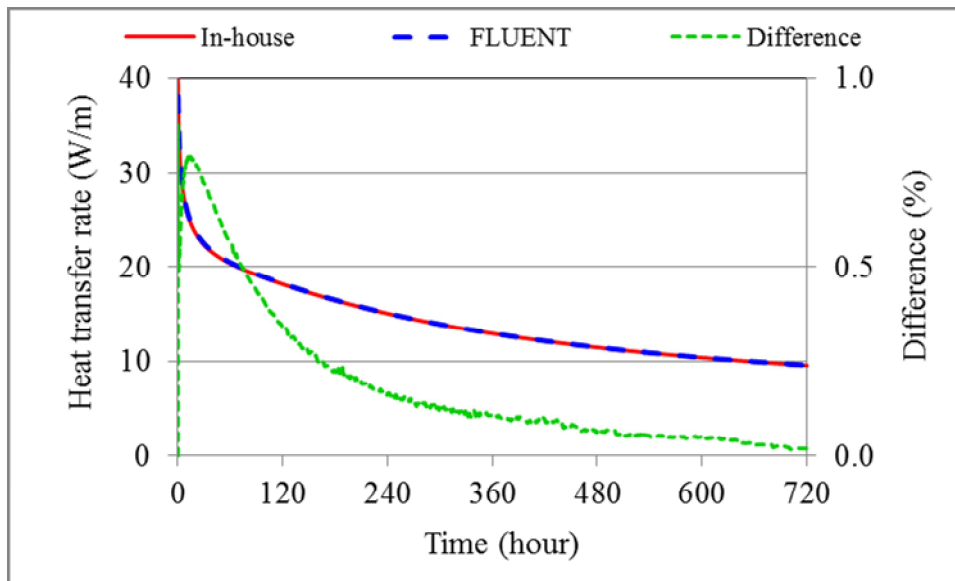


Fig. 3 Predicted heat transfer rate using in-house and FLUENT programs

## 2.5 Simulation conditions

The numerical method is used to assess the performance of an earth-air heat exchanger for preheating of supply air for continuous and intermittent operation in a climate in the Southern England. The heat exchanger is made of high density polyethylene with an external diameter of 200 mm and a wall thickness of 7.7 mm. It is installed horizontally at 1.5 m below the ground surface. Environmental properties are required to account for the interactions not only for supply air inside the heat exchanger but also at the top soil surface. These include the hourly data for air temperature, partial vapour pressure (or wet bulb temperature), solar radiation, cloud cover and wind speed for each month [31] and the monthly rainfall [32]. Values at any time of a day are then calculated from these hourly/monthly data through linear interpolation. The frequency of rainfall is such that it would rain for three hours in evening on every third day. The mean velocity of supply air is 2 m/s at the inlet of the heat exchanger. The soil is of loam texture with 43% sand, 18% clay and 39% silt [33]. Its saturation moisture content is 44% and residual moisture content 5%. The initial moisture content is taken to be one half of the saturation value. The temperature of deep soil is 10°C which can be taken approximately as the annual mean air temperature for the location.

## 3 RESULTS AND DISCUSSION

Simulation has been carried out for two modes of operation - continuous and intermittent. For continuous operation, heat is transferred from soil to air through the heat exchanger at any time of a day when the air temperature is lower than the temperature of the heat exchanger at the inlet opening. For intermittent operation, the heat transfer to air takes place only in a prescribed period of the daytime, again when preheating of supply air is feasible. In other times, heat and moisture transfer still takes place in simulation. However, heat would transfer from soil to the heat exchanger to increase the temperatures of the heat exchanger and surrounding soil as well as static air inside the heat exchanger but not for ventilation. The performance of the heat exchanger is investigated for operation in four months - October, November, December and January - but the discussion is focused on the results for January.

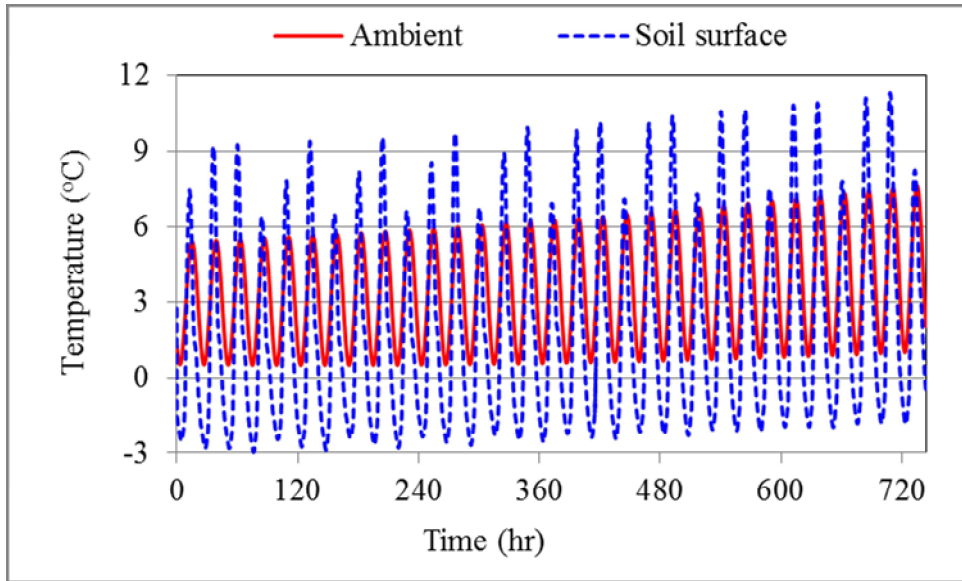
### 3.1 Continuous operation

361 Figure 4 shows the predicted daily variations in ambient air temperature, soil surface  
362 temperature and moisture, and mean moisture for the soil layer between the soil surface and  
363 the crown of the pipe (i.e., heat exchanger) in January. Fig. 5 shows the variations of soil  
364 temperature and moisture along a vertical line through the mid-length and centreline of the  
365 heat exchanger for heating at the end of five typical days. In Fig. 5a, the difference refers to  
366 the temperature difference between the undisturbed (reference) soil and the soil in question.  
367 The soil temperature variation for the first day of October and December is also presented for  
368 comparison of monthly performance later on. The daily air temperature varies by about 5°C  
369 from the minimum of 0.5°C in the early morning (3am) to the maximum of 5.5°C in the  
370 afternoon (3pm) at the beginning of the month. The air temperature rises gradually with the  
371 minimum and maximum to 1°C and 7.6°C, respectively, at the end of the month. The daily  
372 variation of soil surface temperature is much larger mainly because of absorption of solar  
373 radiation during the day and long wave radiation heat loss during the night. The soil surface  
374 temperature drops below the freezing point during much of the night times. The minimum  
375 surface temperature is about -3°C (at 4am) at the beginning (the 2<sup>nd</sup> day) of the month and it  
376 increases to -1.8°C near the end (last but one day) of the month. The corresponding maximum  
377 surface temperature is 9.2°C (at noon) at the beginning and 11.3°C near the end of the month.  
378 The rain in the proceeding night would decrease the soil surface temperature in the following  
379 day due to the lower rainwater temperature (= wet bulb air temperature) and increased  
380 moisture evaporation; e.g., the maximum surface temperature for the 3<sup>rd</sup> and last day of the  
381 month drops to 6.4°C and 8.2°C, respectively.

382  
383 The temperature of the undisturbed soil at 1.5 m deep is about 8°C at the beginning of the  
384 month and decreases to 6.2°C at the end of the month. It is higher than the night time air  
385 temperature. The soil temperature above the heat exchanger is much lower than the deep soil  
386 temperature. At the midnight of the first day, soil temperature 1 m below the heat exchanger is  
387 however still higher than the deep soil. The vertical soil temperature variation is influenced by  
388 the heat exchanger in an area of only 0.6 m from the pipe at the end of the first day, as seen  
389 from the difference in comparison with the temperature of undisturbed soil. During the night  
390 time the soil temperature decreases from heat transfer to the cold ambient at the ground  
391 surface while at any time of a day it would also decrease with operating time due to heat  
392 extraction through the heat exchanger.

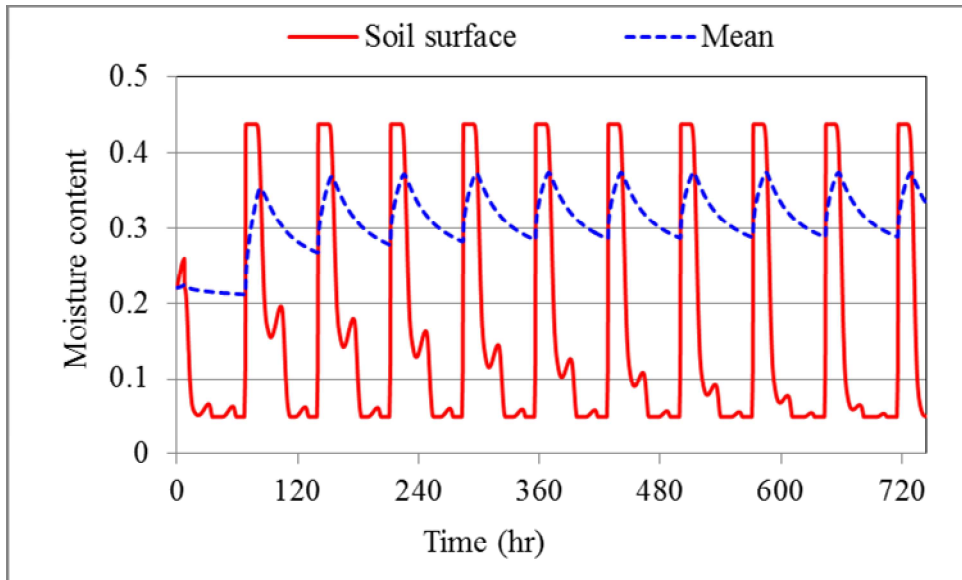
393  
394 Moisture evaporates from the soil during day times. As a result, the surface moisture would  
395 drop rapidly after the sun rises and reach the minimum (residual) value at about 11am and  
396 would remain so till 3 hours after sunset because the evaporation rate would be larger than the  
397 moisture transfer rate from soil below. If it rains in the night before, the soil surface would not  
398 become dry in the following day but the surface moisture would drop to the minimum in the  
399 day after and at a later time from 5pm. During the evening and onwards, the surface moisture  
400 would increase as a result of upward moisture transfer in soil and potential surface  
401 condensation, or frost, if the temperature drops below the dew point, or freezing point,  
402 respectively. Condensation of moisture (or frost formation) on the soil surface occurs as  
403 observed from a slight rise in the moisture content in the first night. The mean moisture for the  
404 soil layer would increase during the rainfall on every third evening and then decrease  
405 afterwards. Overall, the amount of rainfall and moisture condensation exceeds that of surface  
406 evaporation during the first half of the month. This is indicated by the higher mean moisture  
407 from Day 4 than the initial value; the lowest mean is 26.7% on Day 6 before the next round of  
408 rain and 28.4% on Day 15. The soil moisture peaks on Day 15 and remains almost at the same  
409 levels for the rest of the month varying from 28.6% to 37.3% within each rain cycle.

410



411  
412  
413

a) Temperature



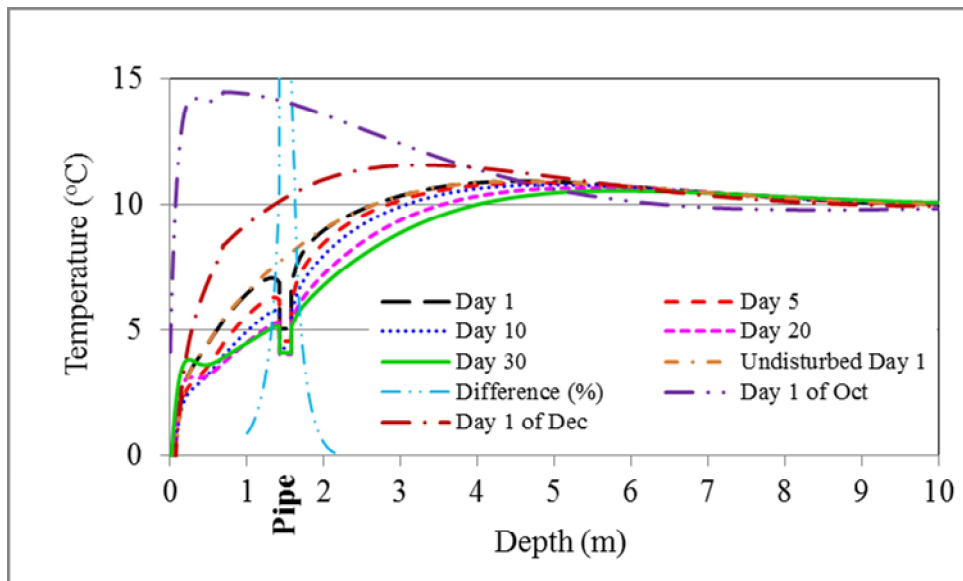
414  
415  
416

b) Moisture content

417 Fig. 4 Predicted daily variations in ambient air temperature, soil surface temperature and  
418 moisture, and mean soil moisture in January

419  
420 In the depth direction, the overall trend of moisture variation is also increasing with time. At  
421 the end of the first day, the moisture variation is limited to the close vicinity of soil surface but  
422 the influence of moisture variation reaches 3.5 m below the soil surface at the end of the  
423 month.

424

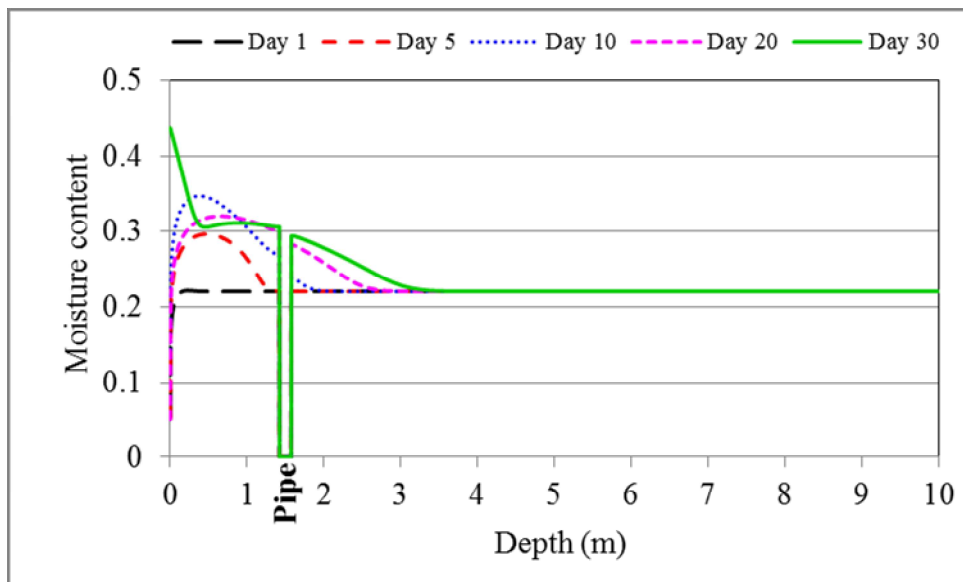


425

a) Temperature

426

427



428

b) Moisture content

429

430

431

Fig. 5 Predicted vertical variations in soil temperature and moisture in January

432

433

### 3.1.1 Variations along the heat exchanger

434

The temperature rise of supply air and the rate and amount of heat transfer through a heat exchanger vary with the length. Simulations have been performed for the heat exchanger with different lengths from 10 m to 40 m in addition to a unit length (1 m).

436

437

438

439

440

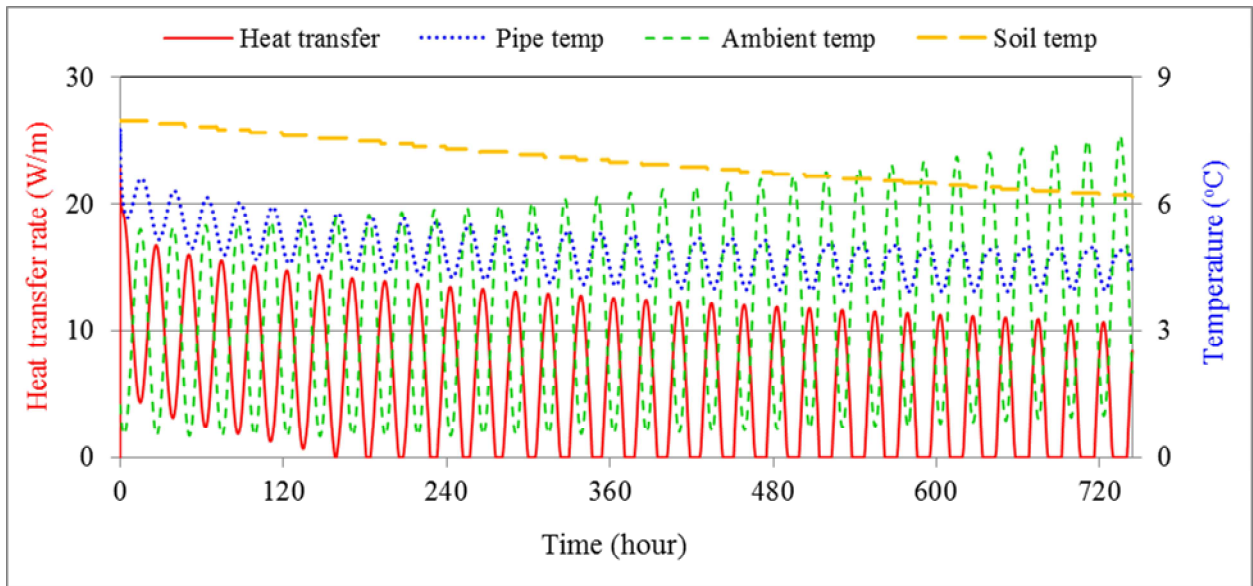
441

442

Figure 6 shows the predicted variations with time in the temperature of the inner pipe surface and heat transfer rate through one pipe of a 10 m long heat exchanger, as well as the ambient air temperature and the temperature of undisturbed soil at a depth of 1.5 m (denoted by soil temp) for reference, for heating in January. The variation in the mean temperature of the 10 m long heat exchanger (defined as the average temperature of the inner surface of the pipe) is



443 much less than that of the ambient air. The daily variation is about 1.4°C compared with 5°C  
 444 to 6.6°C for the ambient air.  
 445



446  
 447 Fig. 6 Predicted variations with time of pipe temperature and heat transfer rate for a 10 m  
 448 long heat exchanger in January

449  
 450 The specific heat extraction, or the heat transfer rate per unit length of the heat exchanger,  
 451 varies with time and with soil and ambient temperatures. Because the soil temperature is more  
 452 stable than air temperature, the specific heat extraction is higher during the night when the air  
 453 temperature is much lower than that in the daytime. The general variation pattern is that  
 454 starting from the midnight the rate of heat transfer increases until at about 3am and then  
 455 decreases to a minimum at about 3pm and finally increases again through the rest of the day.  
 456 For the first day, however, the maximum heat transfer rate of 23 W/m occurs at the beginning  
 457 when the heat exchanger is assumed to be at equilibrium with surrounding soil and the  
 458 temperature difference between the surrounding soil (heat exchanger) and incoming air is thus  
 459 at maximum. The heat transfer rate decreases with decreasing temperature difference to a  
 460 minimum of 4.3 W/m at 3pm on the first day. The rate of heat transfer would decrease day by  
 461 day due to the decreasing soil temperature and from Day 7 the minimum value drops to zero at  
 462 about 2pm when the air temperature becomes higher than the temperature of the pipe inlet.  
 463 This is defined to be the moment when heat in surrounding soil is not available for extraction  
 464 and preheating through the heat exchanger is supposed to stop by means of e.g. by-passing  
 465 ventilating air through the heat exchanger. The duration when heat extraction is not feasible  
 466 increases with operating time from two hours (1pm to 3pm) on Day 7 to 11 hours on the last  
 467 day of the month from 9am to 8pm, i.e., practically no preheating during the daytime.  
 468

469 It should be pointed out that supply air could still be preheated in theory through the heat  
 470 exchanger even if the temperature of ambient air is slightly higher than that of the pipe inlet  
 471 but lower than the average pipe temperature. However, the passing air would be cooled down  
 472 through part of the heat exchanger near the entrance and then heated up in the rest of the heat  
 473 exchanger. Besides, the temperature variation through the length of pipe would be small by  
 474 then. For example, at the time when the air temperature approaches the temperature of pipe at  
 475 the entrance, the temperature increase from the inlet to outlet of a 10 m and a 40 m long heat  
 476 exchangers is only 0.4 K and 1.2 K, respectively, around 2 pm of the 7<sup>th</sup> day (the 1<sup>st</sup> day of the

477 month with a period of time when ambient air temperature is lower than pipe temperature),  
 478 decreasing to 0.3 K and 1.0 K, respectively, around 10 am of the last day of the month.  
 479

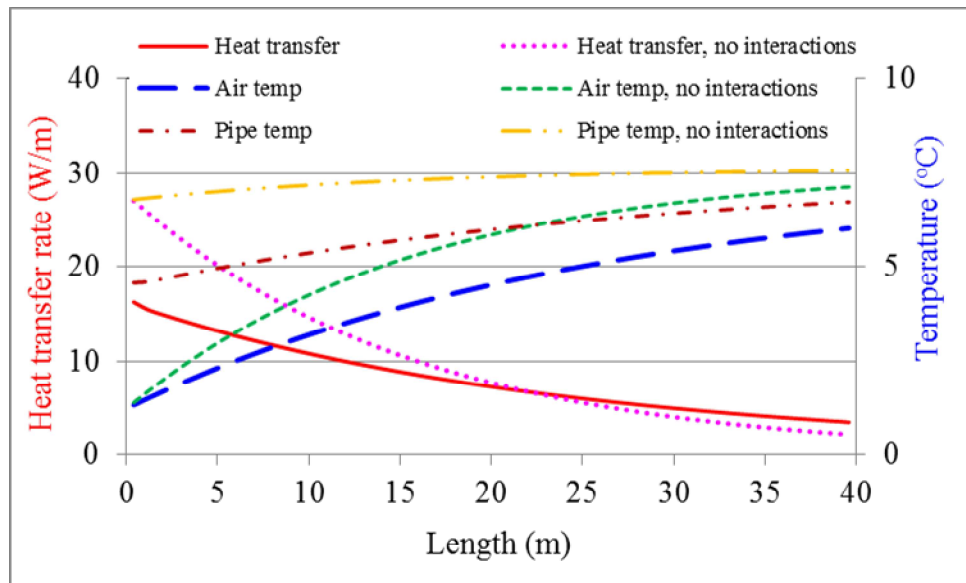
480 The three-dimensional simulations have revealed that temperatures of soil, air and heat  
 481 exchanger and the heat transfer rate also vary with the distance from the inlet along the air  
 482 flow direction (inside the heat exchanger) and that the variations are non-linear. Fig. 7 shows  
 483 the variations in the pipe and air temperatures and heat transfer rate for a 40 m long heat  
 484 exchanger at the end (midnight) of Day 5. The air temperature increases along the heat  
 485 exchanger from 1.3°C at the inlet to 6°C at the outlet because of heat transfer from soil to air.  
 486 The pipe temperature also increases along the heat exchanger from 4.6°C to 6.7°C. The  
 487 increase in the pipe temperature is smaller than that in the air temperature along the air  
 488 passage and thus the temperature difference between the pipe and air (heating potential) is  
 489 much larger near the entrance. The heat transfer rate decreases along the pipe by nearly five  
 490 times from 16.3 W/m at the inlet to 3.5 W/m at the outlet. The magnitude of variations in the  
 491 temperatures and heat transfer with the distance is dependent on the time and duration of  
 492 operation as well as ambient air and soil properties but the variations along the flow passage  
 493 are approximately quadratic. The air and pipe temperatures and heat transfer rate along the  
 494 heat exchanger at the end of Day 5 for example can be represented by the following  
 495 correlations,

496  $T_a = -0.0022 x^2 + 0.202 x + 1.36$   $(R^2 = 0.9993)$  (16)

497  $T_s = -0.00092 x^2 + 0.091 x + 4.53$   $(R^2 = 0.9996)$  (17)

498  $q = 0.0063 x^2 - 0.56 x + 15.94$   $(R^2 = 0.9986)$  (18)

499



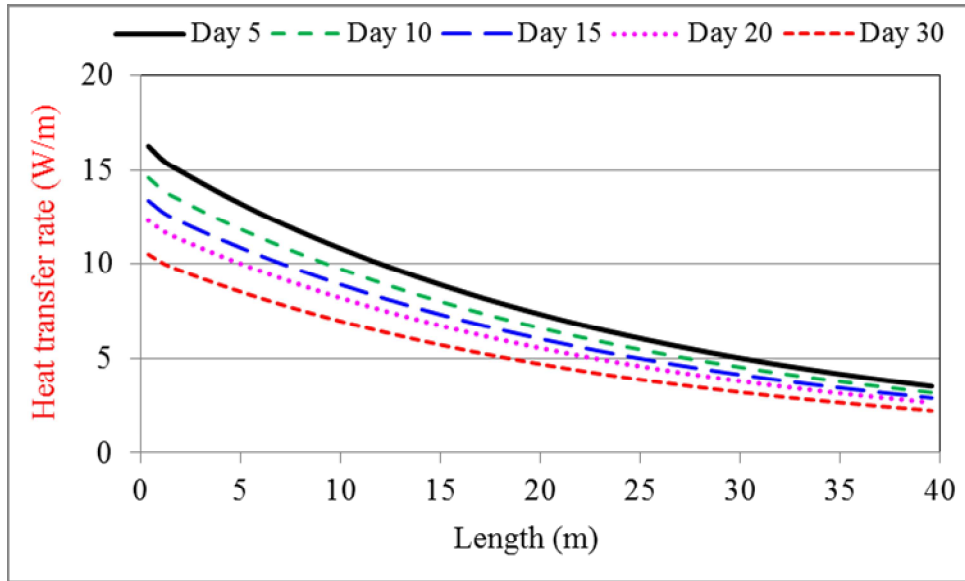
500

501 Fig. 7 Predicted variations of supply air and pipe temperatures and heat transfer rate along the  
 502 pipe length at the end of Day 5

503

504 The variations decrease with increasing operating time as illustrated in Fig. 8 for heat transfer.  
 505 It is also seen that the magnitude of the heat transfer rate decreases with increasing time.  
 506

506



507

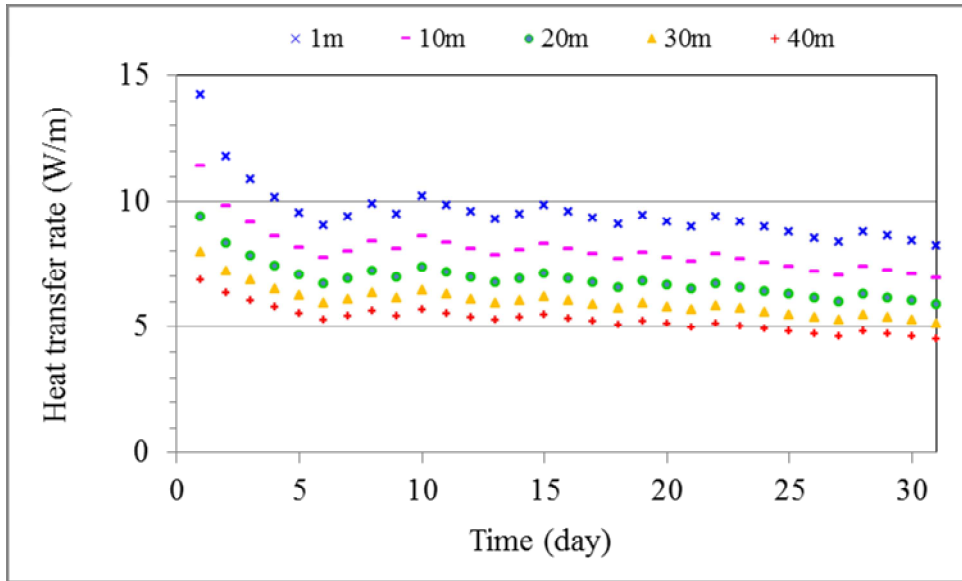
508

Fig. 8 Predicted variation of heat transfer rate along the pipe length

509

510 The results for heat transfer are used to calculate the daily mean values - amount of daily heat  
 511 transfer and mean rate of daily heat transfer. The amount of daily heat transfer (extraction) is  
 512 the cumulative product of the heat transfer rate and time for the duration of heating period and  
 513 the mean rate of daily heat transfer or daily mean heat transfer rate is the average of the heat  
 514 transfer rate for the duration when heat is available for extraction. The daily mean heat transfer  
 515 rate (W/m) and the amount of daily heat transfer (Wh/m) decrease with increasing length as  
 516 shown in Fig. 9. The total heat transfer rate (W) is the product of the mean heat transfer rate  
 517 and the pipe length and this would however increase with length. As a result, the temperature  
 518 of air flowing out of the heat exchanger would depend on the pipe length as well as the  
 519 ambient air temperature. It is seen from Fig. 10a that a 10 m long pipe would be able to reduce  
 520 the daily temperature swing of supply air at the outlet by 1/3 and a 20 m long pipe by 2/3. A  
 521 40 m long pipe would maintain the daily supply air temperature swing within 0.7°C (compared  
 522 with a diurnal ambient air temperature swing of 5 to 6.6°C). The ambient air temperature is  
 523 lower than the undisturbed soil temperature for the first three weeks of the month but higher  
 524 afterwards in some of the day time when preheating of supply air would not be feasible.

525

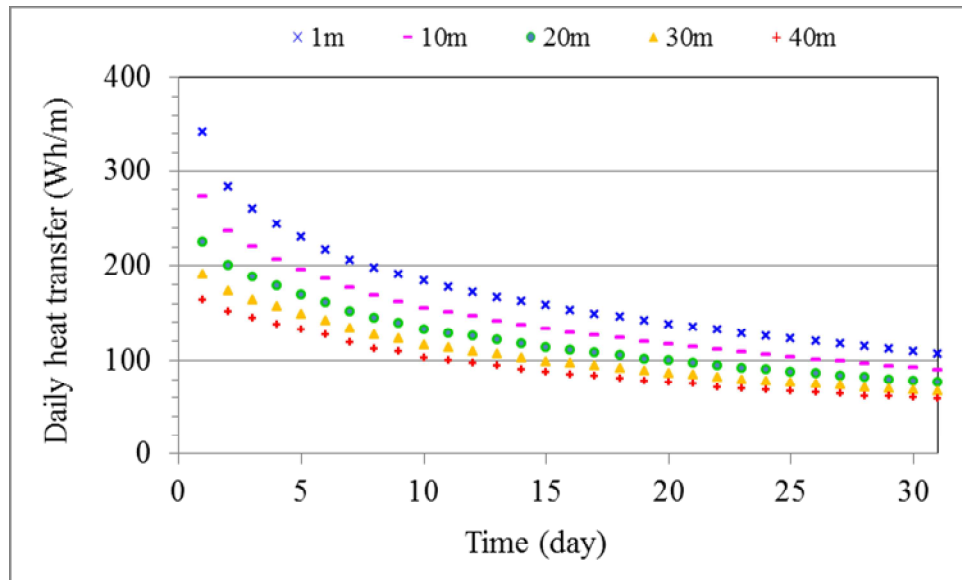


526

527

528

(a) Daily mean heat transfer rate



529

530

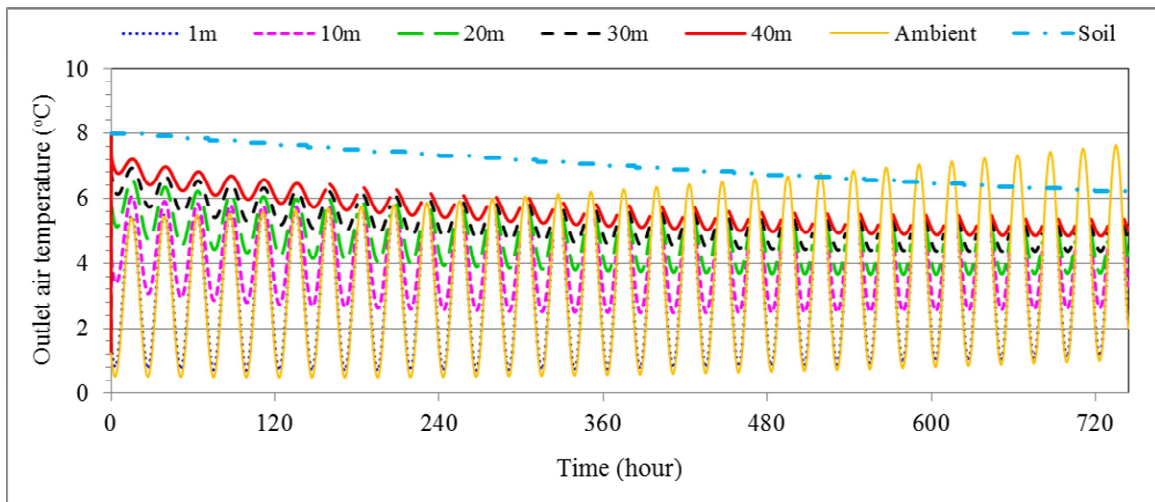
531

(b) Daily heat transfer

532

Fig. 9 Predicted variations of heat transfer with time for different heat exchanger lengths

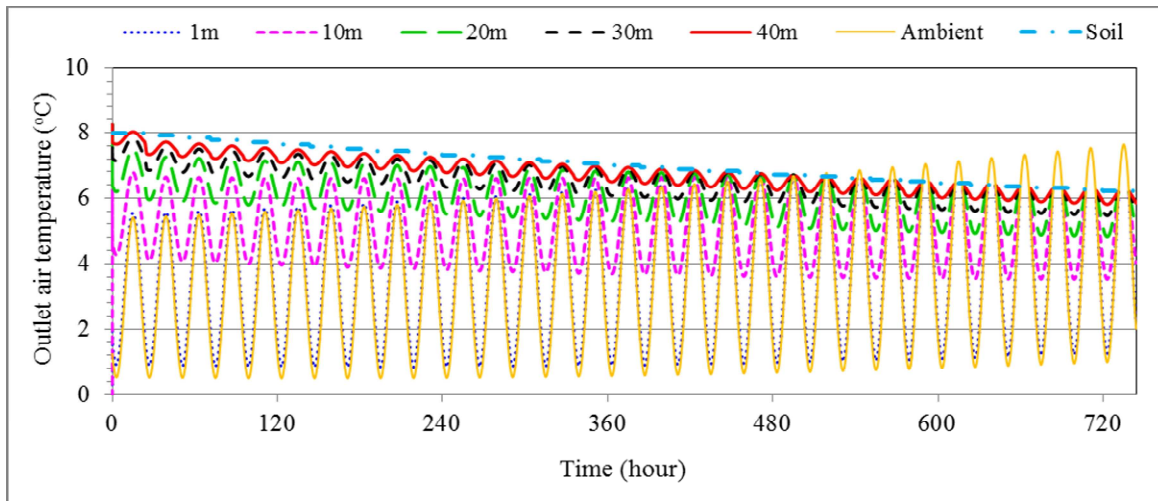
533



534

535

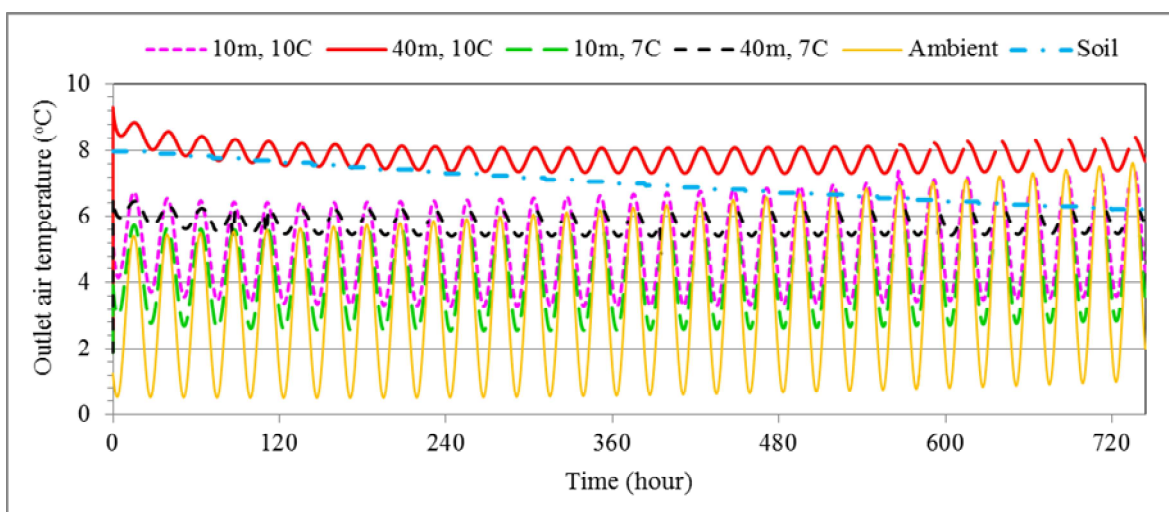
(a) With interactions between the heat exchanger and environments



536

537

(b) With Equation (13) for soil temperature



538

539

(c) With axi-symmetric model for initial soil temperature of 10°C or 7°C

540

Fig. 10 Predicted outlet air temperature for different heat exchanger lengths

541  
542  
543  
544  
545  
546  
547  
548  
549  
550  
551  
552  
553  
554  
555  
556  
557  
558  
559  
560  
561  
562  
563  
564  
565  
566  
567  
568  
569  
570  
571  
572  
573  
574  
575  
576  
577  
578  
579  
580  
581  
582  
583  
584  
585  
586  
587  
588  
589  
590

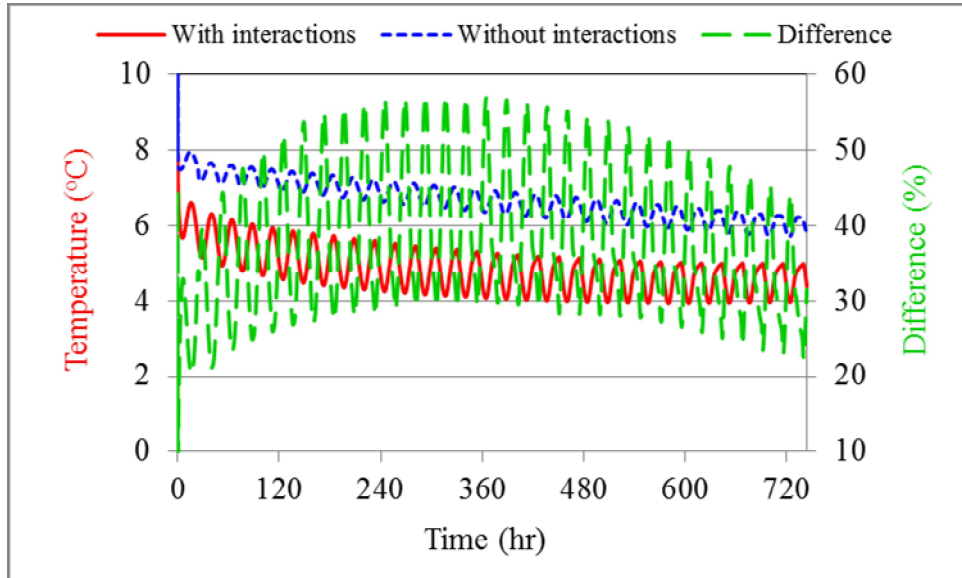
### 3.1.2 Effect of interactions between the heat exchanger, soil and atmosphere

The heat transfer through the heat exchanger is highly influenced by the interactions between the pipe and surrounding soil, between the pipe and supply air inside the pipe, and between soil and atmosphere at the soil surface. Without consideration of these interactions, e.g., the soil temperature at pipe location is given by Equation 13 as used in some of the previous investigations [4 and 5], the predicted heat transfer rate would be much higher because the equation does not take account of the history of heat transfer to air that decreases the soil and pipe temperatures during heat extraction. Fig. 11 shows that, without the cooling effect of supply air, the interior pipe surface temperature is higher but its daily variation is much smaller than those with thermal and moisture interactions between the pipe and soil. The daily pipe temperature swing without considering the interactions is only 0.5°C compared with 1.3°C with interactions. The difference between the two temperature values with and without consideration of the interactions varies all the time each day but overall increases with operating time for the first half of the month and then decreases slightly; the maximum difference occurs on Day 16 with the maximum of 57.2% in the early morning (at around 5am) and the minimum of 29.2% in the early evening (at 7pm) at resumption of heat extraction after the soil temperature recovery period in the daytime when air temperature is higher than the pipe temperature. Fig. 11 also indicates that the difference in the heat transfer rate is larger than that in the temperature and that the peaks and troughs of its daily variation do not follow those of temperature variation. The minimum difference in the heat transfer rate generally occurs at night between 1am and 2am. The difference would be much larger at other times particularly when the air temperature approaches the pipe temperature, leading to negligible heat transfer, during much of the daytime and hence there would be no preheating in the daytime for simulation with consideration of the interactions whereas simulation without considering the interactions would indicate as if heat could be extracted nearly all day long up to Day 21. The highest minimum difference in the heat transfer rate is 60%, found again on Day 16.

The daily amount and mean rate of heat transfer decrease with operating time as shown in Fig. 12. The amount of daily heat extraction decreases because of both decreasing heat transfer rate and operating hours in a day. The difference in the amount or rate of daily heat transfer between the predictions with and without considering the interactions also increases with time up to the middle of the month. The difference in the daily heat extraction predicted with and without consideration of the interactions is larger than that in the heat transfer rate; for example, for the 15<sup>th</sup> day of the month, the predicted daily heat extraction through a 10 m long heat exchanger without considering the interactions is 112% higher than that with full interactions compared with 86% in the heat transfer rate for the same operating period based on the simulation with consideration of the interactions. The larger amount of daily heat transfer without considering the interactions results not only from the predicted higher heat transfer rate but also from the longer time period for heating of supply air – continuous heating for 21 days compared with 6 days only with consideration of the interactions. Note that the presented daily variation in the heat transfer rate is not smooth because the simulated results were recorded hourly for post-processing but the exact period when heat is available for extraction would vary from day to day by minute or second. When the same period for heat extraction, i.e., from 8pm to 9am, is used for processing, the variation becomes smooth as is also shown in Fig. 12a. Note also that the maximum (or minimum) differences for the instantaneous (Fig. 11b) and daily mean (Fig. 12) values could occur in different days (e.g. the 15<sup>th</sup> and 16<sup>th</sup> days).



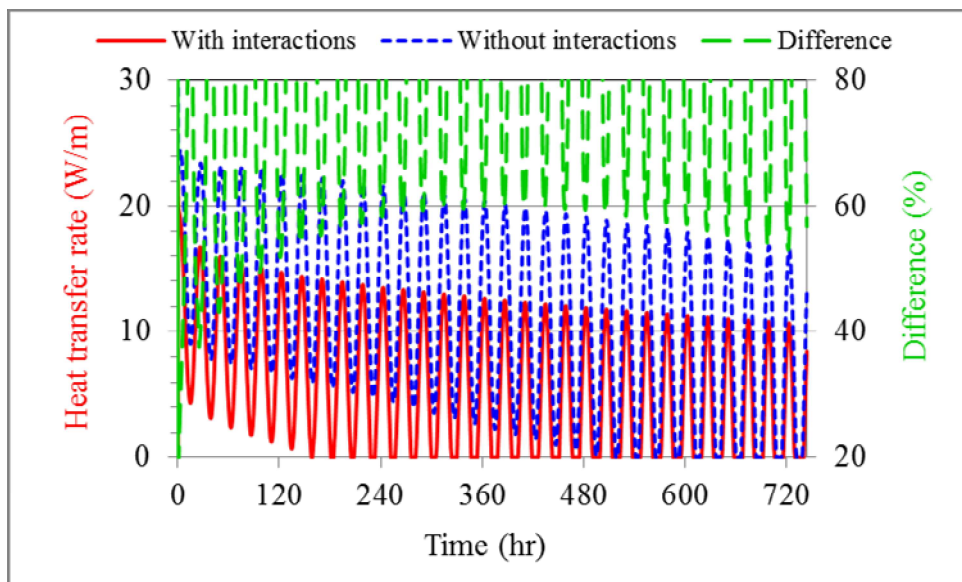
591



592

593

(a) Pipe temperature



594

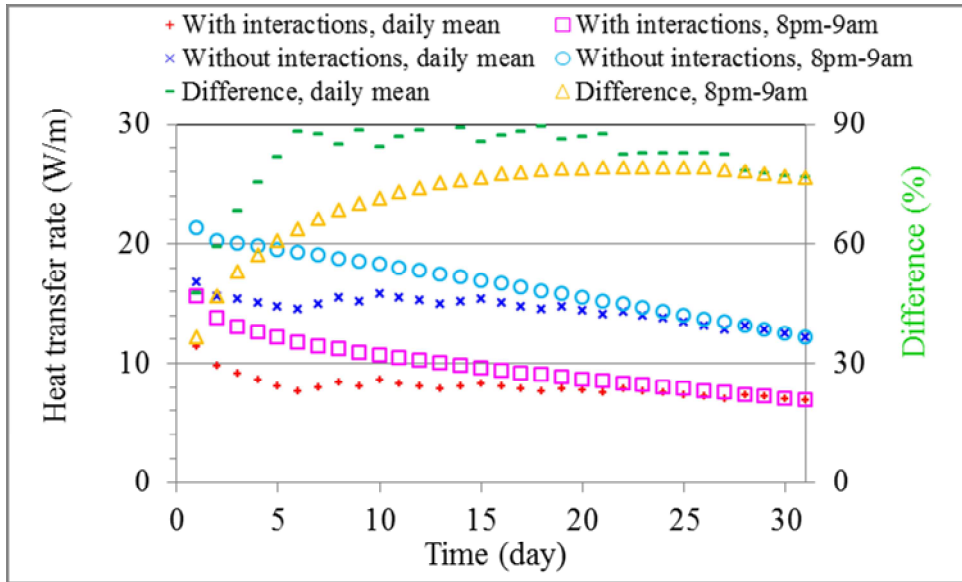
595

(b) Heat transfer rate

596 Fig. 11 Effect of interactions on the predicted variation in pipe temperature and heat transfer  
597 rate for a 10 m long heat exchanger

598 The degree of the interactions between the heat exchanger and the surrounding soil and  
599 atmosphere also varies along the air flow direction in the heat exchanger. These interactions  
600 lead to the increases in air and pipe temperatures but decrease in the heat transfer rate along  
601 the heat exchanger. Neglecting the interactions between the heat exchanger and the soil and  
602 ambient environments, however, the soil temperature given by Equation (13) does not vary  
603 horizontally. The predicted variation in the pipe temperature along the heat exchanger is  
604 therefore smaller but the variation in the air temperature is larger as the potential for heat  
605 transfer is larger near the air entrance. This is indicated in Fig. 7 by the higher heat transfer  
606 rate without considering the interactions compared with the prediction with the interactions for

607 the first half of the pipe length. Also, the decrease in the heat transfer rate along the heat  
 608 exchanger is larger without considering the interactions. As a result, at the end of Day 5, after  
 609 air travels horizontally for about 22 m through the 40 m long heat exchanger, the heating  
 610 potential and heat transfer rate without considering the interactions become smaller than those  
 611 with the interactions. However, the mean heat transfer rate for the whole pipe is still larger  
 612 without considering the interactions than that with the interactions, e.g. 10 W/m compared  
 613 with 8.2 W/m at the end of Day 5 and 6.7 W/m compared with 5.3 W/m at the end of Day 30.  
 614

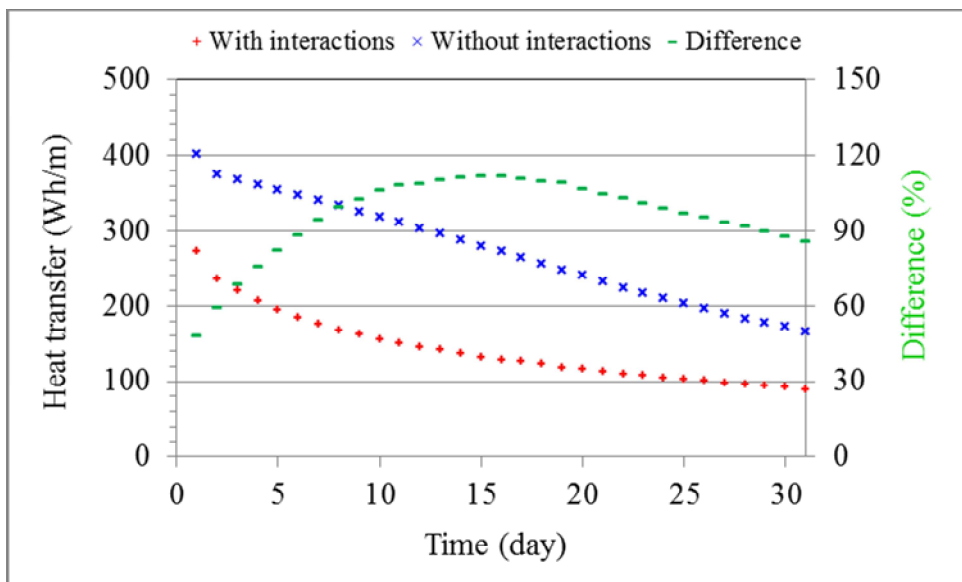


615

616

617

(a) Mean heat transfer rate



618

619

620

(b) Daily heat transfer

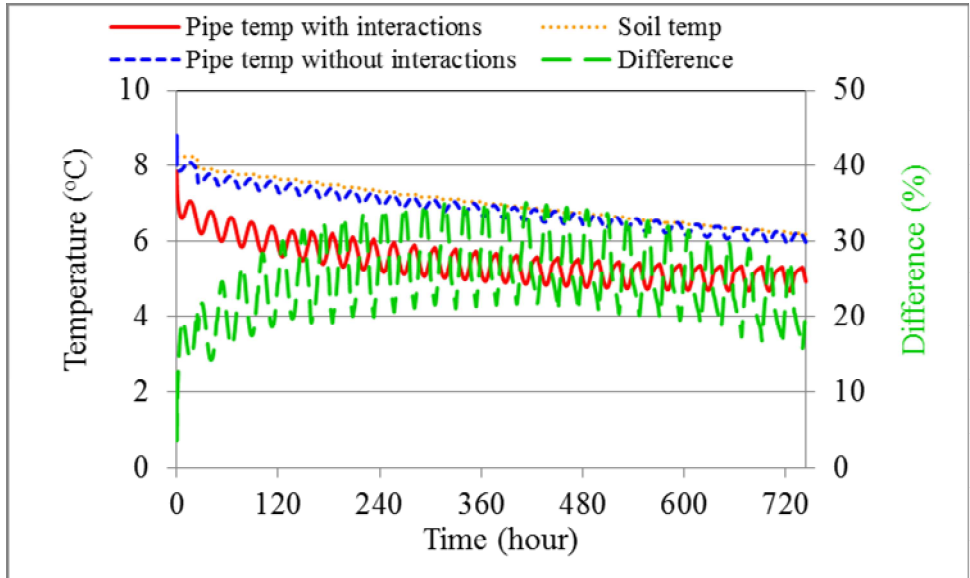
621 Fig. 12 Effect of interactions on the predicted variation in daily heat transfer through a 10 m  
 622 long heat exchanger

623



624 As discussed above, the undisturbed soil temperature is higher than air temperature for most of  
625 days in the month when preheating of supply air would be possible if the interactions between  
626 the heat exchanger, soil and ambient environments were not taken into consideration. By  
627 comparing Fig. 10b with Fig. 10a, it is seen that, without considering the interactions, a 10 m  
628 long pipe could have reduced the temperature difference between soil and ambient air or daily  
629 air temperature swing by  $\frac{1}{2}$  compared with only  $\frac{1}{3}$  with consideration of the interactions and  
630 a 40 m long could have maintained a nearly constant temperature of supply air at the outlet  
631 with a deviation from the soil temperature of less than one half degree (cf  $0.7^{\circ}\text{C}$  with  
632 interactions). However, due to the interactions, the real soil temperature near the heat  
633 exchanger would decrease and the achievable supply air temperature would be lower. Hence,  
634 the error or the difference between the predictions with and without considering the  
635 interactions would increase with operating time for the first half of the month as shown in Fig.  
636 13 for a 40 m long heat exchanger. The difference decreases afterwards because the ambient  
637 air is warming up from then on and the decrease in the pipe surface temperature is slower  
638 when considering the interactions than that without. At the middle of the month (Day 16), the  
639 difference in the predicted pipe temperature for a 40 m long heat exchanger would be between  
640 22.6% for the daytime and 35.4% for the night time. The daily average temperature difference  
641 in supply air between the inlet and outlet, i.e., air temperature rise, through a 40 m long pipe  
642 predicted with and without considering the interactions would be  $3^{\circ}\text{C}$  and  $4.2^{\circ}\text{C}$ , respectively,  
643 a difference of 42%. At the peak of the heat transfer process on the day (3am), the temperature  
644 rise is  $4.4^{\circ}\text{C}$  and  $5.3^{\circ}\text{C}$ , respectively, with and without considering the interactions and the  
645 (minimum) difference is 29%. In other words, neglecting the interactions would over predict  
646 the supply air temperature rise through a 40 m long pipe by as much as  $\frac{2}{5}$ . This is similar to  
647 the difference in the predicted heat transfer rate. The difference in the amount of predicted  
648 heat transfer with and without considering the interactions would be even larger for the  
649 reasons mentioned before. Fig. 14 shows that the difference in the daily mean heat transfer rate  
650 and daily heat transfer would reach 40% and 59%, respectively, at the middle of the month.  
651

652

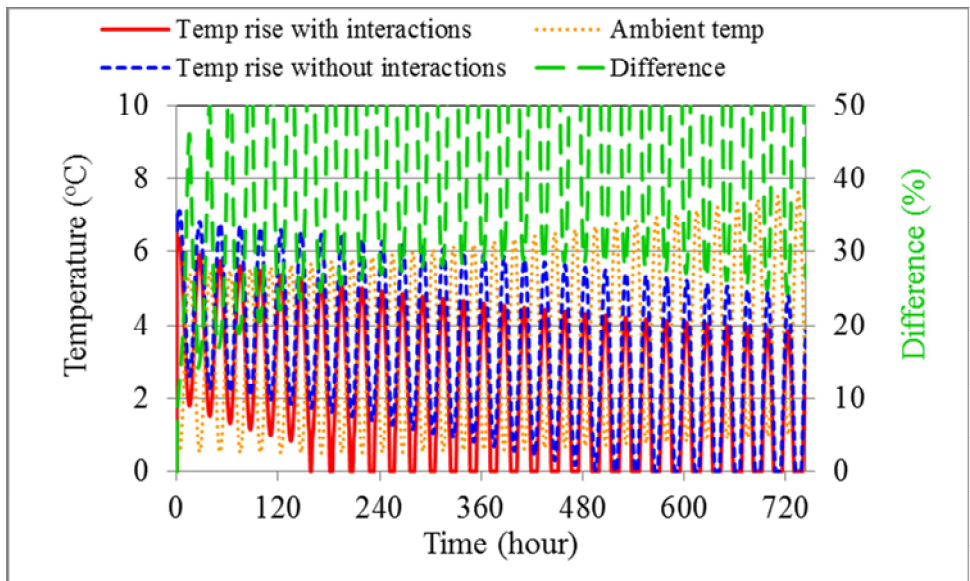


653

654

655

(a) Pipe temperature



656

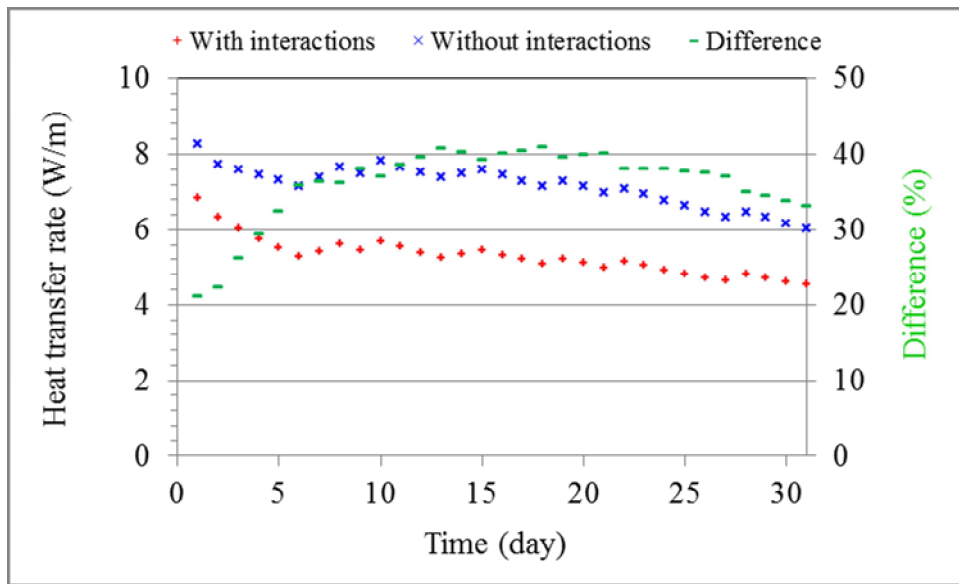
657

658

(b) Temperature increase of supply air

659 Fig. 13 Predicted variations with time of pipe and supply air temperatures for a 40 m long  
660 heat exchanger

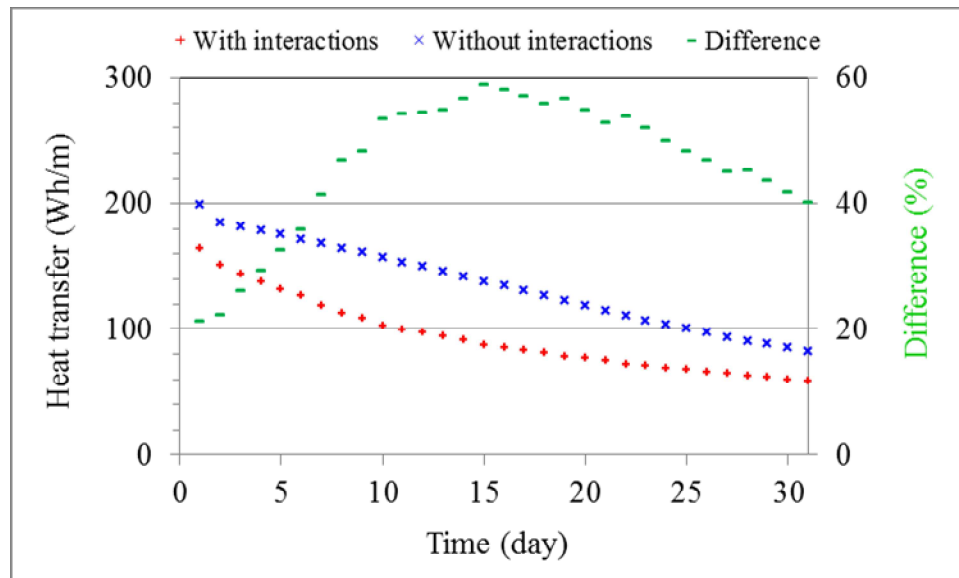
661



662

663

(a) Daily mean heat transfer rate



664

665

(b) Daily heat transfer

666

Fig. 14 Predicted heat transfer for a 40 m long heat exchanger

667

### 668 3.1.3 Effect of interactions between soil and atmosphere

669 Some of the recent studies on the earth-air heat exchanger made use of commercial fluid flow  
 670 software mainly to analyse air flow inside the heat exchanger and heat transfer between the  
 671 heat exchanger and air using an axi-symmetric model [16]. This type of model neglected the  
 672 interactions between soil and atmosphere and spatial variations in thermal and physical  
 673 properties of soil, thus essentially assuming that the heat exchanger would be installed in  
 674 deep soil with uniform properties rather than the shallow ground in practice.

675

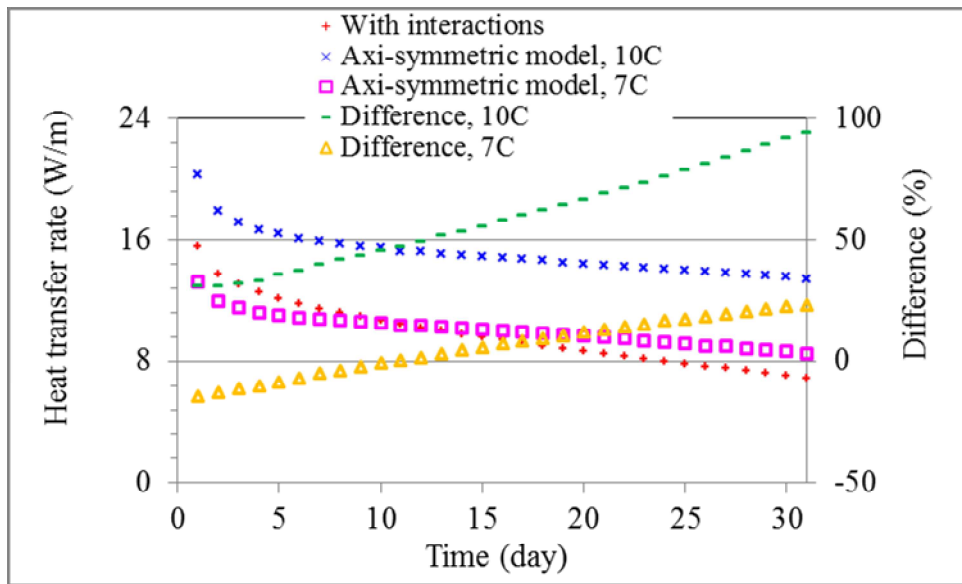
676 To investigate the effect of neglecting the interactions and variations, additional simulations  
 677 have been conducted where the initial soil temperature is set to be uniform as the deep soil

678 temperature ( $10^{\circ}\text{C}$ ) and the heat and moisture transfer at the soil surface as well as far-field  
679 soil boundary is taken to be zero. Meanwhile the heat exchanger is positioned at a great depth  
680 such that there would be no heat transfer across the boundary for the period of operation  
681 investigated. Fig. 15 shows that the heat transfer rate predicted with the axi-symmetric model  
682 is much higher than that predicted with full interactions. This results not only from increasing  
683 daily mean heat transfer rate but also from the excessive heating potential for non-stop  
684 operation for over three weeks. Besides, the percentage difference between the predictions is  
685 almost independent of the length of the heat exchanger, increasing from 31% and 32% for the  
686 10 m and 40 m long heat exchangers, respectively, at the beginning to 94% and 98%,  
687 respectively, at the end of the month. Compared with the predictions using Equation (13) for  
688 the soil temperature, which includes indirectly the influence of varying atmospheric  
689 conditions but takes no account of the interactions between soil and the heat exchanger (Fig.  
690 12 and Fig. 14), the axi-symmetric model would produce much worse results for the (40 m)  
691 long heat exchanger. For the (10 m) short heat exchanger the model could be better for  
692 predicting the performance in early days but eventually it would produce worse results near  
693 the end of the month as well. Moreover, Fig. 10c indicates that the outlet air temperature  
694 either increases with time for a short heat exchanger (to above the likely soil temperature  
695 which is unrealistic) or is almost independent of the time for a long heat exchanger after  
696 operation for a week or so when the soil temperature would in fact decrease with increasing  
697 time for this month. This is because the model could not take account of daily and seasonal  
698 soil temperature variations while employing a varying (increasing on the daily basis) ambient  
699 air temperature. Such results are obviously wrong.

700

701 Of course, the difference could be reduced using a soil temperature closer to operating  
702 conditions such as the temperature at the installation depth. However, as the soil temperature  
703 in the shallow ground varies significantly with time and depth, it is always a hit-and-miss  
704 process. For example, when a soil temperature of  $7^{\circ}\text{C}$  (the mean temperature of undisturbed  
705 soil at the installation depth in January) is used as the far-field value as well as the initial  
706 value, compared with the model including the dynamic interactions, the axi-symmetric model  
707 would under predict the heat transfer rate for the first 10 to 11 days and then over predict the  
708 rate as shown also in Fig. 15. The maximum under-prediction is 15% for the first day and  
709 maximum over-prediction is 23% and 25% at the end of the month for the 10 m and 40 m  
710 long heat exchangers, respectively. The difference between the maximum under- and over-  
711 predictions of heat transfer in one month is between 38% and 40% and the difference would  
712 increase further as operation continues throughout the heating season. In addition, after a few  
713 days' operation, the outlet air temperature would change much on the daily basis and near the  
714 end of the month the air temperature would reach the temperature of undisturbed soil.  
715 Consequently, the model would not be able to predict the day-to-day variation in the  
716 temperature of supply air in trend or magnitude and thus would fail to provide reliable data  
717 for indoor thermal control. Therefore, the model cannot be used for system design or  
718 evaluation of the long term operational performance of an earth-air heat exchanger.

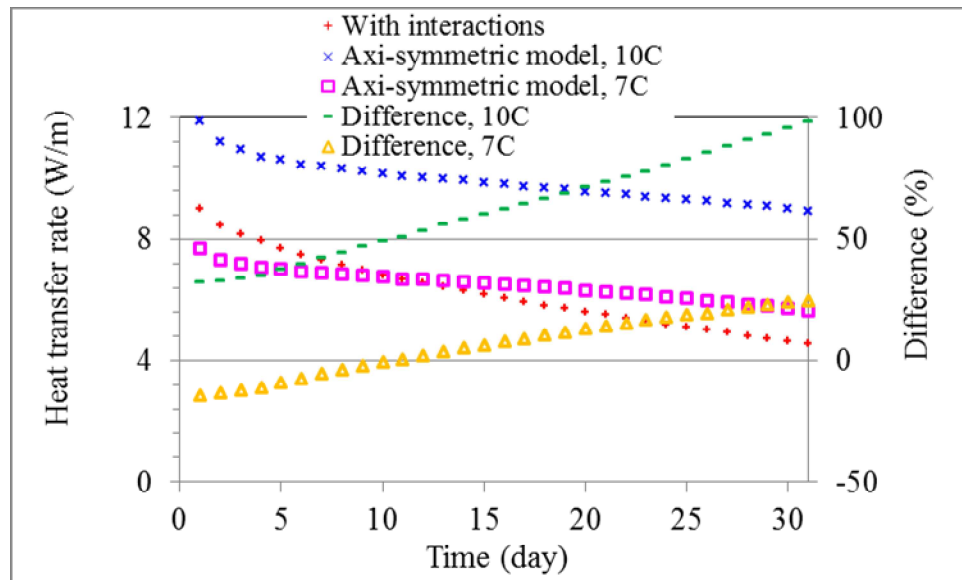
719



720

721

(a) 10 m long heat exchanger



722

723

(b) 40 m long heat exchanger

724 Fig. 15 Comparison of the daily mean heat transfer rate from 8pm to 9am predicted with full  
 725 interactions and with the axi-symmetric model with a deep soil temperature of 10°C or 7°C  
 726

727 An axi-symmetric model for earth-air tunnel ventilation without association with the  
 728 installation depth and the atmospheric conditions at the ground surface is inappropriate, if not  
 729 fundamentally wrong, from the viewpoint of physics and mathematical modelling. The  
 730 validity and reliability of the output is dependent on the inputs such as boundary conditions.  
 731 The soil temperature and moisture in shallow ground are neither uniform nor axi-symmetric  
 732 in most of the times in a year when an earth-air heat exchanger is in operation for preheating  
 733 or cooling of supply air. For example, the soil temperature is generally lower near the ground  
 734 surface in winter but higher in summer than deep soil. The temperature variation along the  
 735 depth is more anti-symmetric than symmetric through the heat exchanger, as shown in Fig. 5.  
 736 Besides, the main source of heat stored in shallow ground is solar radiation and the main

737 processes of heat dissipation from the soil are convection, long wave radiation and  
738 evaporation through the top surface in winter. The heat capacity of shallow ground soil is  
739 therefore influenced much more by the atmospheric conditions than by geothermal energy. In  
740 the axi-symmetric model, however, soil is considered as if it were a giant limitless thermal  
741 reservoir like a geothermal energy source. The model will inevitably fail to predict the long  
742 term thermal performance of a horizontal ground heat exchanger.

743

#### 744 **3.1.4 Monthly performance**

745 The performance of a heat exchanger and the impact of the interactions change not only daily  
746 but also monthly. Fig. 16 shows the predicted daily amount of heat transfer for three months -  
747 October, December and January - for a 40 m long heat exchanger. The heat transfer predicted  
748 with consideration of the interactions increases daily in October for the whole month because  
749 the air temperature decreases faster than does the relatively stable soil temperature and hence  
750 the heating potential – the temperature difference between the heat exchanger and air -  
751 increases. The predicted heat transfer decreases in December as well as January because the  
752 air temperature slowly approaches the minimum in the early December and increases  
753 afterwards. However, in terms of monthly mean performance, a combination of warm soil  
754 and ambient air results in a smaller preheating potential in October than other months  
755 investigated. As air temperature drops faster and further in winter, the preheating potential  
756 reaches the maximum monthly potential in December. The air temperature in January is  
757 actually lower than in December but the soil in the shallow ground is also cold by then.  
758 Consequently, the preheating potential in January is lower than December. The preheating  
759 potential would continue to decrease till the end of heating seasons as air gradually warms up  
760 while the increase in soil temperature lags behind.

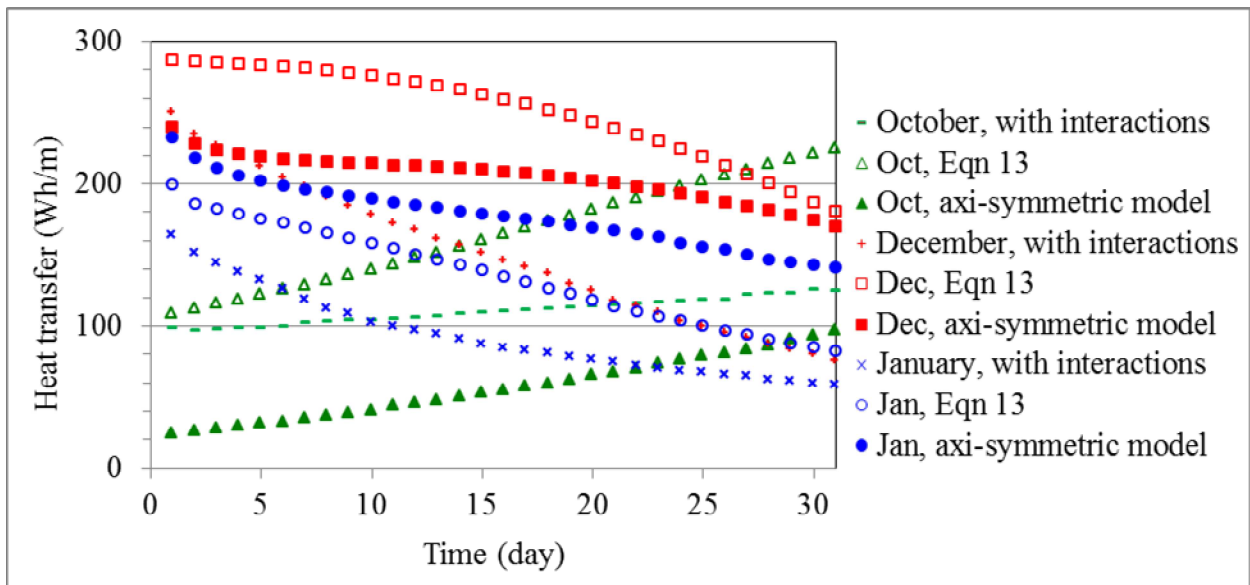
761

762 Neglecting the interactions between the heat exchanger, soil and ventilating air through the  
763 use of Equation (13) would give rise to higher heat transfer for each of the months  
764 investigated. The predicted increase in heat transfer with operating time for October is even  
765 larger without considering the interactions than with consideration of the interactions and the  
766 difference between them also increases with time. By comparison, the predicted heat transfer  
767 for December decreases at a smaller rate without consideration of the interactions than with  
768 the interactions because of the lower rate of the decrease in soil temperature in the first half  
769 of the month and the time lag of the increase in soil temperature in the second half.  
770 Accordingly, the difference between the predictions increases in the first half of the month  
771 and the overall effect of neglecting the interactions using Equation (13) is the largest in  
772 December. The reason for the largest difference for December is because the afore-mentioned  
773 largest heating potential would cool the surrounding soil by the heat exchanger fastest which  
774 could not be taken into account in Equation (13). In terms of the daily heat transfer, the  
775 maximum over-prediction is 72% in the mid-December.

776

777 The level of the difference using the axi-symmetric model compared with the model taking  
778 account of all the interactions is dependent on the deviation of the initial temperature (often  
779 of deep soil) used in simulation from the soil temperature which varies with time and depth.  
780 The model would under predict the thermal performance for periods of time such as October  
781 when the temperature of shallow ground (at the installation depth) is higher than the annual  
782 mean value used for simulation but would otherwise over predict the performance as for  
783 January and all but first few days of December. When the soil temperature differs  
784 significantly from the annual mean value, the under- or over-prediction using the axi-  
785 symmetric model would be much larger than that using Equation (13). For heating in  
786 October, e.g., the difference in the daily heat transfer from the prediction with consideration

787 of all the interactions increases with operating time using both the axi-symmetric model and  
 788 Equation (13). However, using the annual mean temperature for initialisation would lead to  
 789 higher air temperature than soil temperature in the daytime for the whole month and so  
 790 preheating of supply air would only be feasible during night time. The axi-symmetric model  
 791 would thus significantly under predict the performance whereas using Equation (13) would  
 792 over predict the performance. As mentioned above, using Equation (13) would produce larger  
 793 over-prediction for December than that for other months. In contrast, the axi-symmetric  
 794 model would yield similar results to those with consideration of the interactions in the early  
 795 days of this month when the soil temperature at the depth of the heat exchanger happens to be  
 796 close to the annual mean value (see Fig. 5). However, if simulation were continued from  
 797 previous months as likely in practice for heating, the shallow ground would have been cooled  
 798 down by the heat exchanger and the results for these days using the axi-symmetric model  
 799 would also differ significantly from those considering the interactions. Besides, the difference  
 800 for December increases daily and the total difference for the whole month is over 120%, i.e.  
 801 the predicted heat transfer rate at the end of the month using the axi-symmetric model is more  
 802 than double the value predicted with consideration of all the interactions. For January, the  
 803 difference in the daily heat transfer using the axi-symmetric model increases with operating  
 804 time while the difference using Equation (13) peaks in the middle of the month. Thus, the  
 805 level of over-prediction using the axi-symmetric model is much more than that using  
 806 Equation (13).  
 807



808  
 809 Fig. 16 Predicted daily heat transfer for a 40 m long heat exchanger for three months

810  
 811 **3.2 Intermittent operation**

812 As seen from the results for continuous operation, heat extraction from soil may not be  
 813 possible continuously even in the coldest months of the year. Simulations have therefore also  
 814 been performed for two settings of intermittent operation – one for 12 hours for potential  
 815 tunnel ventilation from 8am to 8pm and another for six hours from 8am to 2pm. Accurate  
 816 simulation involving full interactions for intermittent operation is an extremely slow process  
 817 as small time steps have to be used each time the mode of operation is switched in order to  
 818 capture the rapid variations of temperature and moisture with time. Simulation with the soil  
 819 temperature calculated from Equation (13) is however independent of the mode of operation

820 if the effect of heat storage by the heat exchanger is ignored. The axi-symmetric model is not  
821 used for simulation of intermittent operation as it is not suitable for analysis of heat transfer  
822 in shallow ground unless consideration is given to the thermal and moisture interactions with  
823 atmosphere at the soil surface.

824

### 825 **3.2.1 Ventilation between 8am and 8pm**

826 The predicted heat transfer for intermittent operation is compared with that for continuous  
827 operation in Fig. 17. Note that the heat transfer rate at the beginning is very low for  
828 intermittent operation from the equilibrium conditions at 8am (Fig. 17a) whereas the heat  
829 transfer rate at 8am for continuous operation starting from the midnight has already passed its  
830 peak for the day. It is seen from Fig. 17b that the heat transfer rate for intermittent operation  
831 in the daytime is higher than that for continuous operation in the same period of operation for  
832 nine days. However, the heat transfer rate averaged for the operating time for intermittent  
833 operation afterwards decreases to less than the corresponding value for continuous operation.  
834 This is because for continuous operation air temperature would be higher than the pipe  
835 temperature at the inlet during the hours around the noon and heat is not available for  
836 extraction. As a result, the average heat transfer rate during the reduced operating period (e.g.  
837 four hours on Day 15) is higher than that averaged for the 12-hour intermittent operation. Of  
838 course, the rate averaged for the 12 hour period would never be lower for intermittent  
839 operation than that for continuous operation as is seen from the same figure.

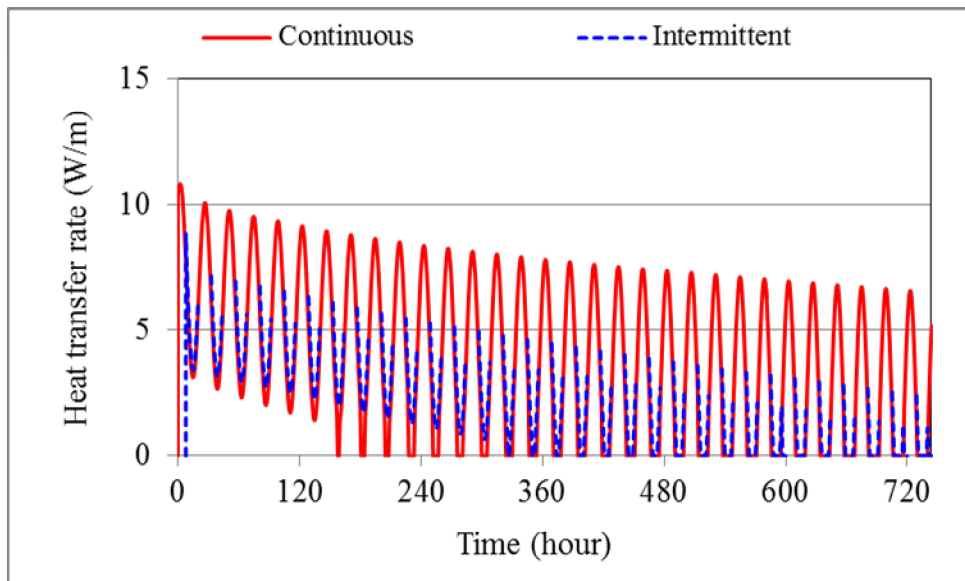
840

841 Even so, the daily mean heat transfer rate predicted without considering the interactions using  
842 Equation (13) is still higher than that with consideration of interactions for intermittent  
843 operation in the same daytime period, increasing from 12% on Day 1 to 40% on Day 10 for a  
844 40 m long pipe (Fig. 18). The difference would be larger for shorter heat exchangers; it is  
845 32% for Day 1 and 84% for Day 10 for a 10 m long heat exchanger. The maximum  
846 difference occurs on Day 18 with 127% and 79% for the 10 m and 40 m long heat  
847 exchangers, respectively. The percentage difference between the predictions with and without  
848 consideration of the interactions is less for intermittent operation than that for continuous  
849 operation in the early days of operation. However, the percentage difference from Day 10 is  
850 larger for intermittent operation than that for continuous operation because the magnitude of  
851 heat transfer during the daytime is lower than that for the night time (comparing Fig. 18 with  
852 Fig. 12 and Fig. 14). For example, on the 10<sup>th</sup> day, the mean heat transfer rate through a 40 m  
853 long heat exchanger for the 12-hour intermittent (daytime) operation (in which mode,  
854 however, heat would not be available for extraction during six hours of the daytime) is 2.8  
855 W/m compared with the mean value of 7.0 W/m for the 12-hour night time for continuous  
856 operation.

857

858



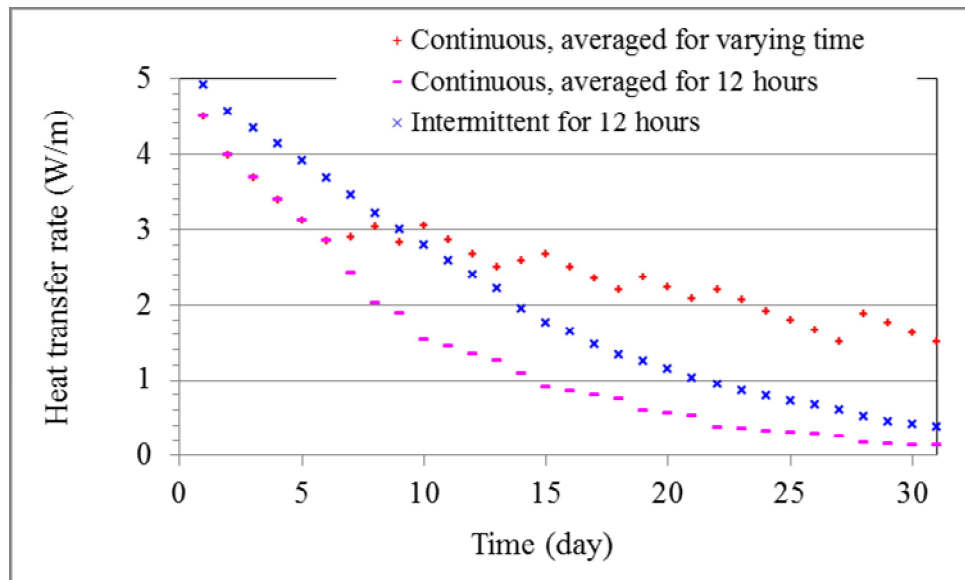


859

860

861

(a) Instantaneous heat transfer rate



862

863

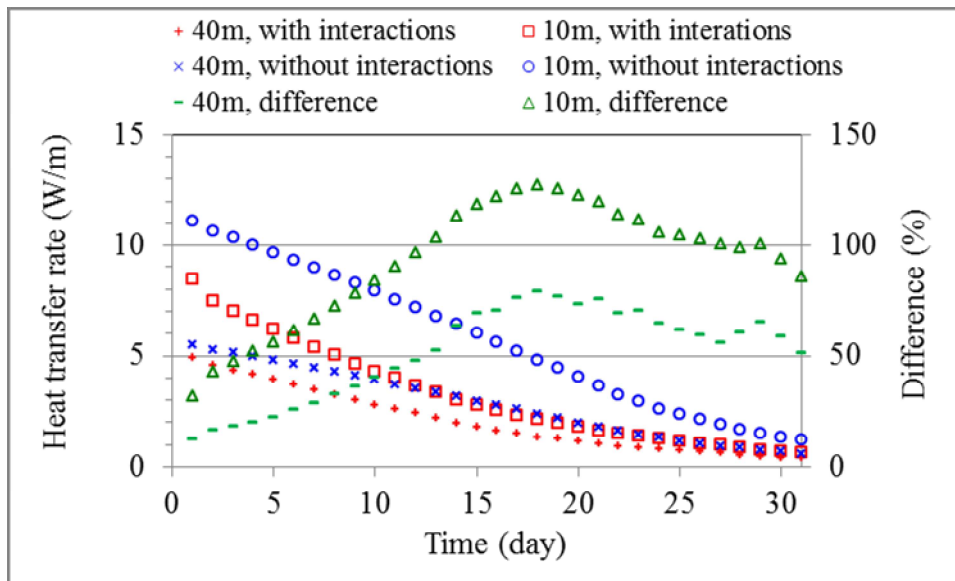
(b) Mean heat transfer rate

864

865

866

Fig. 17 Comparison of the predicted heat transfer rate through a 40 m long heat exchanger between intermittent and continuous operation in January



867

868 Fig. 18 Comparison of the daytime mean heat transfer rate predicted with and without  
 869 interactions for 12-hour intermittent operation in January

870

### 871 3.2.2 Ventilation between 8am and 2pm

872 When the operating period is reduced from 12 hours to six hours, the daily mean heat transfer  
 873 rate per unit length is increased by about 1 W/m and 0.5 W/m for 10 m and 40 m long heat  
 874 exchangers, respectively, for the first half of the month. The percentage increase is almost  
 875 linear from 12% on Day 1 to 25% on Day 15 for the 10 m long heat exchanger and 9% on  
 876 Day 1 to 22% on Day 15 for the 40 m long heat exchanger.

877

878 The difference between the predicted heat transfer with and without considering the  
 879 interactions decreases on average by about 26% to 29% when the operating period is reduced  
 880 from 12 hours to six hours. The percentage difference in the daily mean heat transfer rate for  
 881 6-hour intermittent operation increases from 9% on Day 1 to 28% on Day 10 for a 40 m long  
 882 heat exchanger and from 26% for Day 1 to 62% for Day 10 for a 10 m long heat exchanger.  
 883 The difference increases further, e.g., to 89% and 49% for Day 15 for 10 m and 40 m long  
 884 heat exchangers, respectively. The difference on Day 15 is already higher than that for  
 885 continuous operation. Hence, the maximum percentage difference between the predictions  
 886 with and without consideration of the interactions is still larger for this reduced duration of  
 887 intermittent operation than that for continuous operation.

888

## 889 4 CONCLUSIONS

890 A three dimensional numerical model has been developed for simulation of the dynamic  
 891 thermal performance of earth-air heat exchangers for preheating of supply air. The effects of  
 892 the heat exchanger length and dynamic interactions between the heat exchanger, soil and  
 893 ambient environments have been investigated for continuous and intermittent operation. It  
 894 has been found that the heat transfer rate decreases along the heat exchanger and the rate of  
 895 decrease is non-linear. Consequently, the heat transfer rate and temperature rise of supply air  
 896 per unit length decrease with increasing length of the heat exchanger for preheating.  
 897 However, the overall amount of heat gain and temperature rise of supply air increase with the  
 898 length.

899

900 It has also been found that direct thermal and moisture interactions between a heat exchanger,  
901 soil and atmosphere have a significant impact on the heat transfer through the heat exchanger.  
902 Neglecting the interactions between the heat exchanger and surrounding environments or  
903 between soil and atmosphere would significantly over or under predict the heat transfer rate.  
904 Using an analytical expression for the annual soil temperature variation which neglects the  
905 interactions between the heat exchanger, soil and ventilating air would over predict the  
906 thermal performance of an earth-air heat exchanger. The larger the preheating potential of a  
907 system of ground heat exchanger, soil and atmosphere, the larger the over-prediction. Design  
908 of a building ventilation system based on this method would lead to more in-use heating  
909 energy than predicted. An axi-symmetric model that neglects the interactions between the soil  
910 surface and atmosphere would fail to produce reliable data for long-term operational  
911 performance of the earth-air heat exchanger installed in shallow ground and such a model is  
912 not suitable for system design.

913

914 The impact of over-prediction with regard to long term performance without considering the  
915 interactions is found to be larger for intermittent operation than for continuous operation  
916 when applied to climate conditions such that the potential heat transfer rate is lower in a  
917 period of a day when there is a need for heating than the rest of the day. As intermittent  
918 operation is more likely an operating regime in practice, it is imperative to use dynamic  
919 thermal simulation based on a three-dimensional numerical model that takes account of all  
920 the thermal and moisture interactions in order to provide accurate data for design and analysis  
921 of an earth-air ventilation system.

922

923 The computer program will be used for assessing the effects of other parameters on the  
924 performance of earth-air heat exchangers such as the heat exchanger size, installation depth  
925 and distance between parallel pipes, building load, ventilation rate, type of soil and climate.

926

## 927 **REFERENCES**

- 928 [1]. T.S. Bisoniya, A. Kumar, P. Baredar, Experimental and analytical studies of earth-air  
929 heat exchanger (EAHE) systems in India: A review, *Renewable and Sustainable*  
930 *Energy Reviews* 19 (2013) 238–246.
- 931 [2]. M.D. Paepe, A. Janssens, Thermo-hydraulic design of earth-air heat exchangers,  
932 *Energy and Buildings* 35 (2003) 89–97.
- 933 [3]. K.H. Lee, R.K. Strand, The cooling and heating potential of an earth tube system in  
934 buildings, *Energy and Buildings* 40 (2007) 486–494.
- 935 [4]. V.P. Kabashnikov, L.N. Danilevskii, V.P. Nekrasov, I.P. Vityaz, Analytical and  
936 numerical investigation of the characteristics of a soil heat exchanger for ventilation  
937 systems, *International Journal of Heat and Mass Transfer* 45 (2002) 2407–2418.
- 938 [5]. F. Niu, Y. Yu, D. Yu, H. Li, Heat and mass transfer performance analysis and cooling  
939 capacity prediction of earth to air heat exchanger, *Applied Energy* 137 (2015) 211–  
940 221.
- 941 [6]. R. Kumar, S. Ramesh, S.C. Kaushik, Performance evaluation and energy conservation  
942 potential of earth-air-tunnel system coupled with non-air-conditioned building,  
943 *Building and Environment* 38 (2003) 807–813.
- 944 [7]. O.J. Svec, L.E. Goodrich, J.H.L. Palmer, Heat transfer characteristics of in-ground  
945 heat exchangers, *Energy Research* 7 (1983) 265–278.
- 946 [8]. D. Deglin, L.V. Caenegem, P. Dehon, Subsoil heat exchangers for the air conditioning  
947 of livestock buildings, *Journal of Agriculture Engineering* 73 (1999) 179–188.

- 948 [9]. P. Tittlein, G. Achard, E. Wurtz, Modelling earth-to-air heat exchanger behaviour  
949 with the convolutive response factors method, *Applied Energy* 86 (2009) 1683–1691
- 950 [10]. C. Gauthier, M. Lacroix, H. Bernier, Numerical simulation of soil heat exchanger-  
951 storage systems for greenhouses, *Solar Energy* 60 (1997) 333-346.
- 952 [11]. P. Hollmuller, B. Lachal, Cooling and preheating with buried pipe systems:  
953 monitoring, simulation and economic aspects, *Energy and Buildings* 33 (2001) 509-  
954 518.
- 955 [12]. V.M. Puri, Heat and mass transfer analysis and modeling in unsaturated ground soils  
956 for buried tube systems, *Energy in Agriculture* 6 (1987) 179–193.
- 957 [13]. G. Mihalakakou, M. Santamouris, D. Asimakopoulos, Modeling the thermal  
958 performance of the earth-to-air heat exchangers, *Solar Energy* 53 (1993) 301-305.
- 959 [14]. M. Santamouris, G. Mihalakakou, C. Balaras, A. Argiriou, D. Asimakopoulos, M.  
960 Vallindras, Use of buried pipes for energy conservation in cooling of agricultural  
961 greenhouses, *Solar Energy* 55 (2) (1995) 111–124.
- 962 [15]. J. Darkwa, G. Kokogiannakis, C.L. Magadzire, K. Yuan. Theoretical and practical  
963 evaluation of an earth-tube (E-tube) ventilation system, *Energy and Buildings* 43  
964 (2011) 728–736.
- 965 [16]. V. Bansal, R. Misra, G. Agarwal, J. Mathur, Transient effect of soil thermal  
966 conductivity and duration of operation on performance of earth air tunnel heat  
967 exchanger, *Applied Energy* 103 (2013) 1–11.
- 968 [17]. V. Badescu and D. Isvoranu, Pneumatic and thermal design procedure and analysis of  
969 earth-to-air heat exchangers of registry type, *Applied Energy* 88(4) (2011) 1266–  
970 1280.
- 971 [18]. J. Vaz, M.A. Sattler, E.D. Dos Santos, L.A. Isoldi, Experimental and numerical  
972 analysis of an earth-air heat exchanger, *Energy and Buildings* 43(9) (2011) 2476–  
973 2482.
- 974 [19]. V. Khalajzadeh, M. Farmahini-Farahani, G. Heidarinejad, A novel integrated system  
975 of ground heat exchanger and indirect evaporative cooler, *Energy and Buildings* 49  
976 (2012) 604–610.
- 977 [20]. A. Flaga-Maryanczyka, J. Schnotale, J. Radon, K. Was, Experimental measurements  
978 and CFD simulation of a ground source heat exchanger operating at a cold climate for  
979 a passive house ventilation system, *Energy and Buildings* 68 (2014) 562–570.
- 980 [21]. J. Wang, N. Christakis, M.K. Patel, M.C. Leaper and M. Cross, A computational  
981 model of coupled heat and moisture transfer with phase change in granular sugar  
982 during varying environmental conditions, *Numerical Heat Transfer – Part A* 45 (2004)  
983 751–776.
- 984 [22]. D.Q. Yang, H. Rahardjo, E.C. Leong and V. Choa. Coupled model for heat, moisture,  
985 air flow and deformation problems in unsaturated soil, *Journal of Engineering*  
986 *Mechanics* 124(12) (1998) 1331-1338.
- 987 [23]. R. Katsman and R. Becker, Model for moisture-content evolution in porous building  
988 elements with hygro-thermal bridges and air-voids, *Journal of Building Physics* 20  
989 (2000) 10-41.
- 990 [24]. G. Gan, Effect of combined heat and moisture transfer on the predicted indoor thermal  
991 environment, *Indoor + Built Environment* 5(3) (1996) 170-180.
- 992 [25]. G. Gan, Dynamic interactions between the ground heat exchanger and environments in  
993 earth–air tunnel ventilation of buildings, *Energy and Buildings* 85 (2014) 12–22.
- 994 [26]. R.B. Clapp, G.M. Hornberger, Empirical equations for some soil hydraulic properties,  
995 *Water Resources Research*, 14 (1977) 601-604.
- 996 [27]. G. Gan, Dynamic thermal modelling of horizontal ground source heat pumps,  
997 *International Journal of Low Carbon Technologies* 8(2) (2013) 95-105.

- 998 [28]. G. Gan, CFD simulation for sustainable building design, in: R. Yao (ed), Design and  
999 Management of Sustainable Built Environments, Springer-Verlag, London, 2013, pp.  
1000 253-277.
- 1001 [29]. Y. Wu, G. Gan, A. Verhoef, P.L. Vidale, R. Garcia Gonzalez, Experimental  
1002 measurement and numerical simulation of horizontal-coupled slinky ground source  
1003 heat exchangers, Applied Thermal Engineering 30(16) (2010) 2574-2583.
- 1004 [30]. ANSYS Inc. FLUENT, Canonsburg, Pennsylvania, 2010.
- 1005 [31]. CIBSE, Guide J - Weather, solar and illuminance data, Chartered Institution of Building  
1006 Services Engineers, London, 2002.
- 1007 [32]. UK Climate, <http://www.metoffice.gov.uk/public/weather/climate/bracknell>.  
1008 Accessed on April 5, 2013.
- 1009 [33]. B.J. Cosby, G.M. Hornberger, R.B. Clapp, T.R. Ginn, A statistical exploration of the  
1010 relationships of soil moisture characteristics to the physical properties of soils, Water  
1011 Resources Research 20(6) (1984) 682-690.